Journal of
Medicinal Plant Research
Volume 10 Number 26, 10 July, 2016
ISSN 1996-0875

Academic Journals

ABOUT JMPR

The Journal of Medicinal Plant Research is published weekly (one volume per year) by Academic Journals.

The Journal of Medicinal Plants Research (JMPR) is an open access journal that provides rapid publication (weekly) of articles in all areas of Medicinal Plants research, Ethnopharmacology, Fitoterapia, Phytomedicine etc. The Journal welcomes the submission of manuscripts that meet the general criteria of significance and scientific excellence. Papers will be published shortly after acceptance. All articles published in JMPR are peer reviewed. Electronic submission of manuscripts is strongly encouraged, provided that the text, tables, and figures are included in a single Microsoft Word file (preferably in Arial font).

Contact Us

Editorial Office: jmpr@academicjournals.org

Help Desk: helpdesk@academicjournals.org

Website: http://www.academicjournals.org/journal/JMPR

Submit manuscript online http://ms.academicjournals.me/

Editors

Editorial Board

Journal of Medicinal Plants Research

Table of Contents: Volume 10 Number 26 10 July, 2016

ARTICLES

academicJournals

Vol. x(xx), pp. xxx xx, xxxxx, 2016
DOI:10.5897/JMPR2016.XXXX
Article Number: xxxxxxxxxx
ISSN 1996-0875

http://www.academicjournals.org/JMPR

Journal of Medicinal Plants Research

Full Length Research Paper

Liver damage in an experimental model of peripheral neuropathy induced by *Karwinskia humboldtiana* (Buckthorn) fruit: Histopathological evidence

Rubén García-Garza[1], Martha E. Salazar-Leal[2], Viktor J. Romero-Díaz[3], Jaime García-Juárez[3], Carlos Leyva-Orasma[4], Javier Morán-Martínez[5], Odila Saucedo-Cárdenas[3,6] and Adolfo Soto-Domínguez[3]*

[1]Departamento de Histología, Facultad de Medicina, Universidad Autónoma de Coahuila, Unidad Torreón. Av. Gregorio A. García 198 Sur, Torreón, Coah. México. C.P. 27000.
[2]Departamento de Farmacología y Toxicología. Facultad de Medicina. Universidad Autónoma de Nuevo León. Monterrey Nuevo León. A.P. 1583. México.
[3]Departamento de Histología. Facultad de Medicina. Universidad Autónoma de Nuevo León. Monterrey Nuevo León. A.P. 1583. México.
[4]Universidad Autónoma Agraria Antonio Narro, Periférico Raúl López Sánchez y Carretera a Santa Fé, C.P 27054, Torreón, Coah, México.
[5]Departamento de Biología Celular y Ultraestructura, Centro de Investigación Biomédica, Universidad Autónoma de Coahuila, Unidad Torreón. Av. Gregorio A. García 198 Sur, Torreón, Coah. México. C.P. 27000.
[6]Centro de Investigación Biomédica del Noreste (CIBIN), IMSS, San Luis y 2 de Abril. Col. Independencia. Monterrey, N.L. México. C.P. 64720.

Received 2 February, 2016; Accepted 19 April, 2016

***Karwinskia humboldtiana* (*Kh*) is a poisonous shrub that causes acute or chronic intoxication in animals and humans. In chronic intoxication, the main sign is the presence of paralysis. Previously we reported a model of intoxication with *Kh* fruit that reproduces paralysis and clinical phases in humans when they do not die; however, there are no studies that describe damage to liver in this model. The objective was to evaluate histopathological alterations in liver during chronic intoxication. Wistar rats (n=25) were divided into five groups (n= 5). Four groups were intoxicated with *Kh* and one received only water as a control group. Animals were euthanized at different times during paralysis evolution. Samples of liver were obtained, and processed either for light or electron microscopy evaluation. Histological, histochemistry and immunohistochemistry analyses were performed, including a morphometric analysis. Results demonstrated necrotic areas, vascular congestion and vacuoles in the cytoplasm of hepatic cells that increased during intoxication and decreased in the recovery stage. These findings were confirmed at electron microscopy level. Morphometric analysis demonstrated statistically significant difference in occurrence of necrotic cells and PCNA positive cells between control and intoxicated groups. This was not observed with TUNEL staining. These findings demonstrate that during *Kh* intoxication there is a severe damage in liver that is reversible. Thus, it could be suggested that *Kh* causes a systemic intoxication not only damage to peripheral nervous system.**

Key words: *Karwinskia humboldtiana,* plant intoxication, liver damage.

INTRODUCTION

Karwinskia humboldtiana (Kh) also known as tullidora, capulín tullidor or coyotillo, is a poisonous shrub from the *Rhamnaceae* family. It is distributed throughout the Mexican Republic, South America, Central America and Northern of Colombia (Fernández, 1992). Dreyer et al. (1975) isolated from the endocarp of *Kh* four dimeric anthracenonic compounds named as T-496, T-514, T-516 and T 544, according to their molecular weights, which have been demonstrated to be responsible for the toxicity of this plant (Dreyer et al., 1975; Waksman et al., 1989, Rivas et al., 1990; Bermúdez et al., 1992, Waksman and Ramirez, 1992).

In the literature, there are numerous reports of accidental human intoxications with *Kh* fruit (Castillo et al., 1920; Segovia et al., 1972; Bustamante et al., 1978; Puértolas et al., 1984; Arellano et al., 1994; Bermudez et al., 1995; Ocampo et al., 2007). Clinical sign of this intoxication varies according to the amount of fruit ingested. In acute intoxication, respiratory failure and death may occur within 2 to 3 days without paralysis signs. If it is consumed in small quantities or chronic intoxication, after a few weeks of consumption, a clinically flaccid, symmetrical, ascending and progressive paralysis appears which can lead to death (Segovia et al., 1972); or in some cases human can recover slowly from the paralysis (Arellano et al., 1994).

Acute intoxication of Wistar rats with *Kh* fruit has shown liver disorders and clotting characterized by an increase in aspartate transaminase (AST) and alanine transaminase (ALT), as well as a decrease in II, V, VII and X coagulation factors (Jaramillo et al., 2009). Only there are two *in vitro* studies in hepatocytes of rat treated with *Kh* fruit (Wheeler et al., 1971), or with T-514 (Garza-Ocañas et al., 2003) that reported mitochondrial alterations and increase of toxic oxygen radicals. *In vivo* experimental studies of acute toxicity with purified toxin T-514 administered to different species have reported atelectasis and emphysema, along with infiltration of polymorphonuclear cells in alveolar septa, rupture of capillaries and bleeding (Bermúdez et al., 1986; Sepúlveda et al., 1992). In liver, congestion and massive necrosis were reported, especially with T-514 (Bermudez et al., 1986).

Salazar et al. (2006) reported a model of chronic intoxication with *Kh*, by the administration of fractionated doses of mature fruit of this plant to Wistar rat. This model reproduces the clinical phases of paresis, paralysis, and recovery that are presented in intoxicated humans when they do not die (Salazar et al., 2006). Recently, we demonstrated a toxic effect of *Kh* fruit on striatum of Wistar rat using this same intoxication model (Díaz-Pérez et al., 2016). Since there have not been found any studies that describe damage to organs like the liver in this model, the objective was to evaluate histopathological alterations in this organ during chronic intoxication with the fruit of *Kh.*

MATERIALS AND METHODS

Study groups and administration of Kh fruit

Wistar rats (n=25) were used, and all animals were divided into five groups (n = 5). Four groups where intoxicated with fruit of *Kh* according to the intoxication model described by Salazar et al. (2006), and one only received water as control animals; all the animals were kept under standard laboratory conditions. Experiments were carried out according to the International Guidelines on the Appropriate use of Experimental Animals, and according to Mexican Norm NOM-062-ZOO-1999 on the Technical Specifications for Production, Care and Use of Laboratory Animals (SAGARPA, 1999). The protocol was approved by the Bioethical Committee of the Faculty of Medicine UANL in Monterrey, Nuevo León, México.

After a period of 6 h of fasting, rats to intoxicate received a fractionated dose of dry, ground, and sieved fruit of *Kh* that was dissolved in water and orally administered through an orogastric tube. The first dose was of 1.5 g/kg (Day 0) followed by four subsequent doses of 0.5 g/kg at days 3, 7, 10 and 14 after the first dose (total dose of 3.5 g/kg). Control rats received only water and all rats were clinically evaluated during the experimental study time according to intoxication model described by Salazar et al., (2006). Weight was determined daily during the first two weeks, every third day from third to eighth week, and weekly from eighth week until the end of the study at day 112 post-intoxication. The clinical evaluation included the appearance of piloerection, spontaneous mobility, muscle tone, gait abnormalities, respiratory rate, weight loss, limb weakness and paralysis.

Sample collection

Animals of all study groups were sacrificed by cervical dislocation at the corresponding days after the intoxication as follows: First group was sacrificed at day 24 post-intoxication before the rats presented paresis (group without paresis). Second group was sacrificed at day 48 post-intoxication when rats had paresis (paresis group). Third group corresponded to intoxicated rats showing paralysis at day 58 (paralysis group), and finally the recovery group corresponded to the intoxicated rats that showed clinical recovery from paralysis and were sacrificed at day 112 post-intoxication.

Histopathological analysis

Liver samples were obtained, fixed by immersion in formalin 10 % in PBS (Phosphate Buffer Saline) 1X, pH 7.2-7.4 and processed by routine histological technique until inclusion of samples in paraffin blocks. Histopathological evaluation was performed on sections of 5-7 µm thickness. Sections were stained with hematoxylin and eosin (H&E) for histopathological evaluation, Masson´s trichrome to detect connective tissue, and silver impregnation to identify reticular fibers (collagen type III). This was performed as follows 5 µm

*Corresponding author. E-mail: ibqasoto@yahoo.com.mx. Fax: 52-82-8348-5477.

paraffin sections were hydrated and then oxidized with 1% potassium permanganate. They were rinsed well with tap water, bleached in 5% oxalic acid for a 1 min and sensitized with 1% uranium nitrate solution for 5-10 s. Later, they were rinsed with distilled water, treated with Bielchowsky's ammoniacal silver for 1 min (48 mL of 2% silver nitrate) and 0.4 mL of 40% sodium hydroxide was added. While swirling, slowly drops of strong ammonium hydroxide were added until the precipitate dissolved. They were put in 100 mL of distilled water and then rinsed briefly with 90% ethanol. They were placed in the developer (5 ml of 37% formalin, 0.15 g uranium nitrate and 1L of distilled water) for 1 min and rinsed well with tap water and distilled water. Then, they were toned with 0.2% gold chloride solution and rinsed with distilled water. Also, they were fixed in 5% sodium thiosulphate for 1 min and washed well with running tap water. They were counterstained with eosin for 1 min and rinsed with tap water. Finally, they were dehydrated with ethanol, cleared with xylene and mounted onto a resinous medium.

Histochemistry

A portion of formalin-fixed tissue was processed for frozen section technique. Histological sections of 6-8 µm thickness were obtained, and stained with Oil Red technique for the histochemistry identification of lipids droplets deposits.

Immunohistochemical evaluation

To distinguish between morphological necrotic alterations induced by *Kh* intoxication from apoptotic hepatocytes, the TUNEL (TdT-mediated dUTP-biotin Nick-End Labeling) test was performed on 6-8 µm thick sections to detect fragmentation of nuclear DNA, a hallmark of apoptosis (Gavrieli et al., 1992) using the kit TACS™ 2 TdT *In situ* Apoptosis Detection of Trevigen® (Gaithersburg, MD. USA), according to the instructions of the manufacturer. Nuclei were contrasted with methyl green.

Furthermore, to determine whether *Kh* intoxication inhibits proliferation of liver cells, histological sections (4-5 µm thick) were incubated with anti-PCNA (Proliferating Cell Nuclear Antigen) monoclonal antibody (1: 200) to identify proliferating cells (Matsumoto et al., 1987; Zhang et al., 1999) using the Envision® detection system and 3, 3'diaminobenzidine (DAB). PCNA antibody and the detection system were purchased from Dako Cytomation, Inc® (Carpinteria, Ca. USA). Nuclei were contrasted with Mayer´s hematoxylin. As a negative control, the monoclonal antibody was omitted. The samples were analyzed by light microscope.

Morphometric analysis

To quantify necrotic hepatocytes, the liver parenchyma was divided in hepatic acini or liver Rappaport acini. Hepatic acini (zones 1, 2 and 3) or Rappaport´s hepatic acinus represents a liver lobule that is divided into 3 regions based on their proximity to the distributing veins: zone I has cells closest to the vessels (portal triad) and first to be affected by incoming blood with toxins, zone II with cells which are second to respond to toxic compounds in blood (in between portal triad and central vein), and zone III with cells near the central vein. Quantization was performed in 24 random fields per group (eight fields/slide, one slide/rat, three rats/group) were chosen from sections stained with H&E and observed with the oil immersion objective (100X). In these fields the normal and necrotic hepatocytes in the 3 zones described for the hepatic acini were quantified.

This methodology was also applied to quantify positive cells to TUNEL test and to PCNA antibody. Digital high-resolution images were obtained with a Nikon Microscope Eclipse 50i, and with the image analysis system Digital Sight dDS-2Mu. Averages and standard deviations (SD) were calculated, and a student´s t-test was performed with the statistics software SPSS program v.16 to compare the control *vs* experimental groups, a value of $p \leq 0.05$ was considered as statistically significant.

Ultrastructure

Simultaneously, other portion of liver was fixed by immersion in solution of Karnowsky-Ito (4% paraformaldehyde, 5% glutaraldehyde, and 0.05% picric acid in 0.1 M PBS pH 7.2-7.4) (Ito and Karnowsky; 1968). Samples were post fixed in 2% aqueous osmium tetroxide, and processed by conventional technique for transmission electron microscopy until their inclusion in epoxy resins to form blocks. Semithin and ultrathin sections were obtained by ultramicrotomy; semithin sections were stained with 1% toluidine blue and analyzed by light microscopy. Ultrathin sections were mounted on copper grids 200 mesh without support medium, and contrasted with 5% uranyl acetate followed by 0.04% lead citrate; samples were analyzed with a Zeiss EM 109 transmission electron microscope.

RESULTS

Clinical manifestations

Clinical manifestations, such as weight loss, ocular secretion, hair bristling, weakness, and respiratory difficulty, were analyzed in rats intoxicated with *Kh* fruit. These manifestations were present in the paresis group at 48 days, were more evident at 58 days in the paralysis group, and almost all of the symptoms resolved in the recovery group, which only presented piloerection (Table 1).

Histopathogical evaluation

In the control samples hepatocytes, portal triads, central venous and sinusoids with normal histological features were observed (Figure 1A). In groups without paresis and with paresis, vascular congestion and small cytoplasmic vacuoles in most hepatocytes were observed (Figure 1B and 1C). In these groups we also observed areas of necrotic hepatocytes characterized by hyperchromatic nucleus and extracted cytoplasm. In the paralysis group, generalized vascular congestion, large cytoplasmic vacuoles in most hepatocytes (Figure 1D), as well as larger amount of necrotic areas of hepatic cells were observed. Finally, in recovery group, most of the alterations described above were absent; only vascular congestion was observed (Figure 1E).

With the method of Masson´s trichrome, in all groups few blue collagen fibers were observed around the central veins, and portal triads with normal characteristics (Figure 2A-2E). Signs of fibrosis were not observed. Also, in control and intoxicated groups, with the silver impregnation it was possible to identify thin reticular fibers without differences among all groups (Figure 3A-

Table 1.

Clinical manifestations	Without Paresis (24 days)	Paresis (48 days)	Paralysis (58 days)	Recovery (112 days)	Related organ	Histopathological findings
Weight loss	+	+	++	-	Liver (Present Study)	Steatosis, necrosis of hepatic cells.
Respiratory difficult	+	++	+++	+	Lung (García- Garza et al., 2013)	Fibrosis in interalveolar septum, presence of mast cells.
Ocular secretion	+	+	++	-	Peripheral nerve (Salazar et al., 2006, García- Garza et al., 2013)	Segmental demyelination in some fibers, swelling and myelin sheath vacuolization. Axonal alterations such as alternating thinned and thickened zones.
Hair bristling	+	+	++	-	Peripheral nerve (Salazar et al., 2006, García- Garza et al., 2013)	Segmental demyelination in some fibers, swelling and myelin sheath vacuolization. Axonal alterations such as alternating thinned and thickened zones.
Weakness	+	+	+++	-	Peripheral nerve (Salazar et al., 2006, García- Garza et al., 2013) Brain (Díaz-Pérez et al., 2016)	Segmental demyelination in some fibers, swelling and myelin sheath vacuolization. Axonal alterations such as alternating thinned and thickened zones. Neuronal damage.
Decreased spontaneous activity	+	+	++	-	Peripheral nerve (Salazar et al., 2006, García- Garza et al., 2013) Brain (Díaz-Pérez et al., 2016)	Segmental demyelination in some fibers, swelling and myelin sheath vacuolization. Axonal alterations such as alternating thinned and thickened zones. Neuronal damage.
Alopecia of eyebrows	+	+	++	-	Peripheral nerve (Salazar et al., 2006, García- Garza et al., 2013)	Segmental demyelination in some fibers, swelling and myelin sheath vacuolization. Axonal alterations such as alternating thinned and thickened zones.
Alopecia of dorsal region	+	+	++	-	Peripheral nerve (Salazar et al., 2006, García- Garza et al., 2013)	Segmental demyelination in some fibers, swelling and myelin sheath vacuolization. Axonal alterations such as alternating thinned and thickened zones.
Walk alterations	-	+	++	-	Peripheral nerve (Salazar et al., 2006, García- Garza et al., 2013) Brain (Díaz-Pérez et al., 2016)	Segmental demyelination in some fibers, swelling and myelin sheath vacuolization. Axonal alterations such as alternating thinned and thickened zones. Neuronal damage.
Muscular atrophy	-	+	++	-	Peripheral nerve (Salazar et al., 2006, García- Garza et al., 2013)	Segmental demyelination in some fibers, swelling and myelin sheath vacuolization. Axonal alterations such as alternating thinned and thickened zones.

Table 1 cont'd

General sickness	-	+	++	-	Liver (Present Study) Lung (García- Garza et al., 2013a) Kidney (García Garza et al., 2013b	Fibrosis in interalveolar septum, presence of mast cells, steatosis, necrosis in uriniferous tubules, damage to filtration slits.
Spinal deformity	-	+	++	-	Peripheral nerve (Salazar et al., 2006, García- Garza et al., 2013) Brain (Díaz-Pérez et al., 2016)	Segmental demyelination in some fibers, swelling and myelin sheath vacuolization. Axonal alterations such as alternating thinned and thickened zones. Neuronal damage.
Claw hand	-	-	+	-	Peripheral nerve (Salazar et al., 2006, García- Garza et al., 2013)	Segmental demyelination in some fibers, swelling and myelin sheath vacuolization. Axonal alterations such as alternating thinned and thickened zones.
Paralysis	-	-	+	-	Peripheral nerve (Salazar et al., 2006, García- Garza et al., 2013) Brain (Díaz-Pérez et al., 2016)	Segmental demyelination in some fibers, swelling and myelin sheath vacuolization. Axonal alterations such as alternating thinned and thickened zones. Neuronal damage.
Polineuropathy disappears	-	-	-	+	Peripheral nerve (Salazar et al., 2006, García- Garza et al., 2013)	Remyelination of peripheral nerve.
Improvement of the general condition	-	-	-	+	Liver (Present study) Peripheral nerve (Salazar et al., 2006)	Liver recovery , remyelination of peripheral nerves.

-: Absent, +: Mild, ++ : Severe

3E).

Histochemistry evaluation

In the control samples, lipids were not present in the cytoplasm of hepatocytes demonstrated with oil red (Figure 4A). Groups without paresis and with paresis showed a diffuse positivity to this reaction in the cytoplasm in extended areas of hepatocytes (Figure 4B and 4C); deposits of lipids were more evident in the samples of paralysis group (Figure 4D). In recovery group little lipids droplets remained in the cytoplasm of hepatocytes (Figure 4E).

Immunohistochemical evaluation

By the TUNEL assay, few positive cells to chromatin fragmentation were observed in control group and experimental groups (Figure 5A-5E). By immunohistochemical analysis of PCNA, the highest number of proliferating cells was observed in control group (Figure 6A); followed by groups without paresis (Figure 6B) and with paresis (Figure 6C). It is noteworthy that group with paralysis showed fewer positive cells (Figure 6D), recovery group showed higher number of positive cells compared with the other treated group

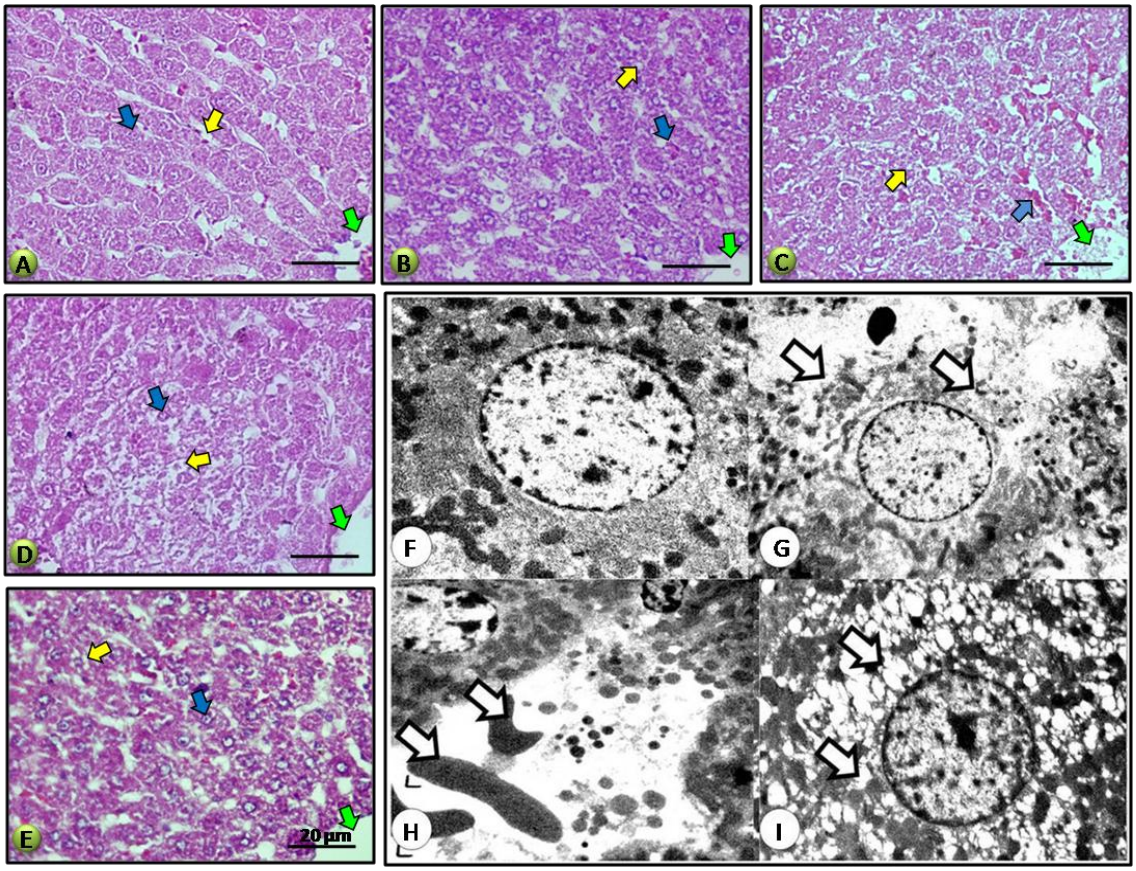

Figure 1. *Kh induces necrotic alterations in hepatocytes in intoxicated groups:*A) Control group with normal histology: nuclei (blue arrow), sinusoids (yellow arrow), central vein (green arrow). B-D) Groups without paresis, paresis and paralysis, respectively, showing vascular congestion (blue arrow), increasing cytoplasmic vacuoles and necrotic alterations in hepatocytes (yellow arrow), central vein (green arrow). E) Recovery group shows most of hepatocytes with normal appearance, only small cytoplasmic vacuoles remained (yellow arrow). H&E. Bar: 20 µm. *Hepatic ultrastructural alterations induced by Kh fruit:* F) Hepatocyte of control group with normal ultrastructural appearance. In intoxicated groups following alterations were observed: G) hepatic necrosis with loss of continuity of the cell membrane and cytoplasmic extraction (arrow), H) vascular congestion in the sinusoidal lumen (arrow), I) vacuolization of the cytoplasm of hepatocytes (arrows). Inclusion in epoxy resins. Transmission electron microscope, F: 7000×, G-I: 4400×.

(Figure 6E).

Morphometric analysis

In the morphometric analysis of liver acini (zones 1, 2 and 3), control group showed only a few hepatocytes damaged per field of view (2,583 ± 1,127; 2,850 ± 0,476 and 1,800 ± 0,519). In the group without paresis, more altered hepatocytes were observed (19,900 ± 2,351; 23,600 ± 5,567 and 17,183 ± 2,133). In paresis group, increased damaged hepatocytes (29,933 ± 4,623; 34,667 ± 1,607 and 34,833 ± 1,985). However, paralysis group presented the highest number of necrotic damage (50,333 ± 4,523; 61,867 ± 2,400 and 61,167 ± 2,478), recovery group showed 8,233 ± 2,315; 8,833 ± 2,182 and 9,633 ± 0,416. Statistical analysis revealed a significant difference in intoxicated group compared with control group (Figure 7A).

The number of positive nuclei in TUNEL analysis in the control group was 2.978 ± 1.321, while in the groups intoxicated with *Kh* the results are as follows: group without paresis (4.159 ± 0.888), paresis group (4.344 ± 0.432), paralysis group (5.122 ± 0.992) and recovery (3.233 ± 1.523), respectively. When comparing the results of control *vs* treated groups no significant difference was found for a value of p≤0.05 (Figure 7B).

In proliferation analysis (the number of PCNA positive cells) in control and treated groups, it was observed that control group showed the highest number of positive cells: 26,110 ± 0,639, group without paresis had 22.185 ± 1.054, then paresis group with an average of 18.245 ± 0.732. Group with paralysis showed the lowest amount of positive cells with an average of 12.503 ± 0.521, and

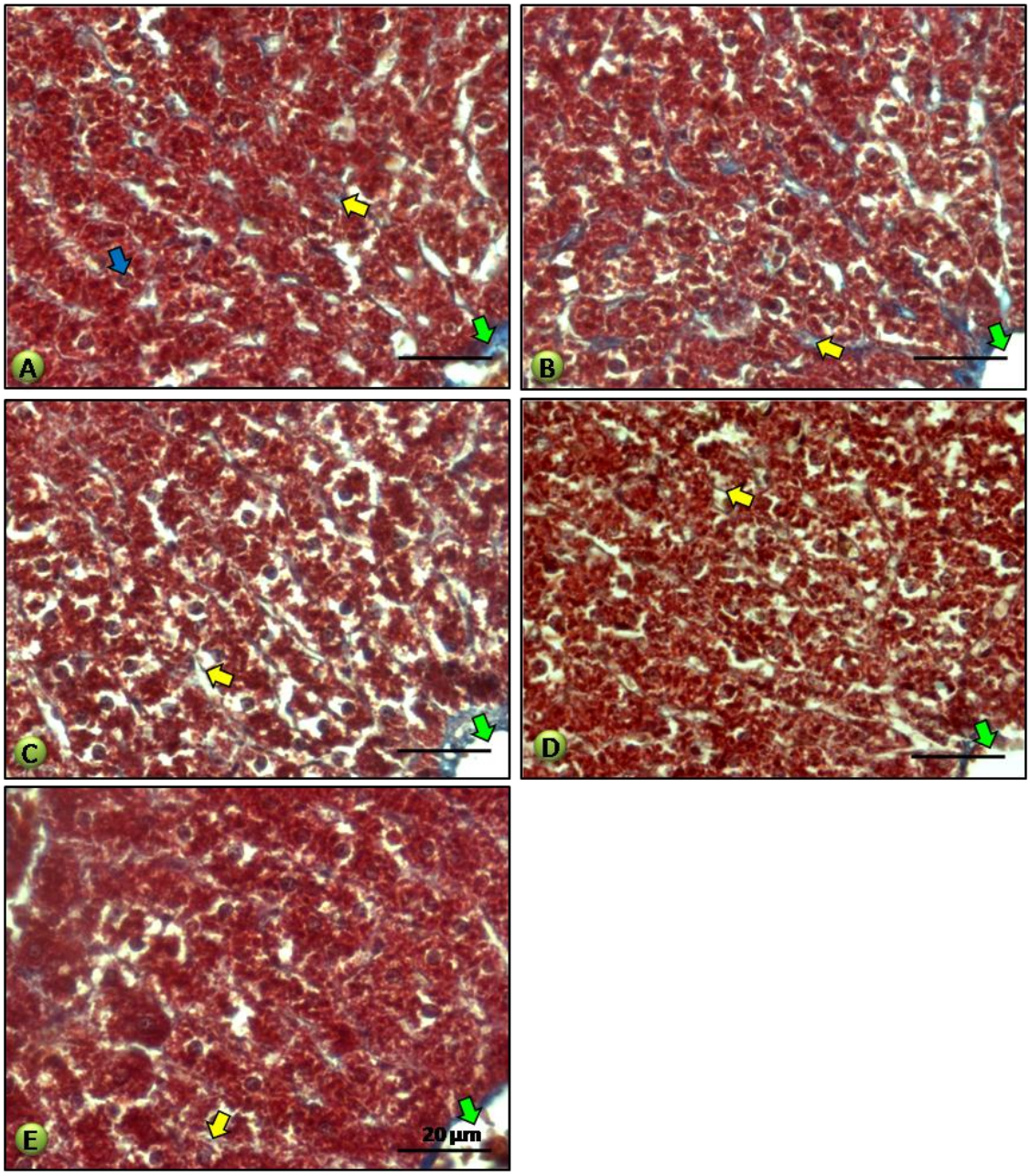

Figure 2. *Kh does not causes fibrosis :*A) Control group with normal histology: nuclei (blue arrow), collagen fibers (yellow arrow), central vein (green arrow). B-E) intoxicated groups showing collagen fibers similar to control group, collagen fibers (yellow arrow), central vein (green arrow). Masson`s trichrome. Bar: 20 µm.

finally recovery group showed an amount of 19.024 ± 3,792. All treated groups intoxicated with *Kh* were significantly different from the control group ($p \leq 0.05$; Figure 7C).

Ultrastructural evaluation

In control samples hepatocytes were observed with the cell membrane, nucleus and organelles with normal ultrastructural features (Figure 1F). In groups without paresis and with paresis, necrotic hepatocytes with loss of the continuity of the cell membrane and cytoplasmic extraction (Figure 1G) were observed, as well as sinusoids with vascular congestion (Figure 1H). In these same groups other hepatocytes were observed with small spaces in the cytoplasm corresponding to extracted lipids (Figure 1I). In paralysis group these alterations increased

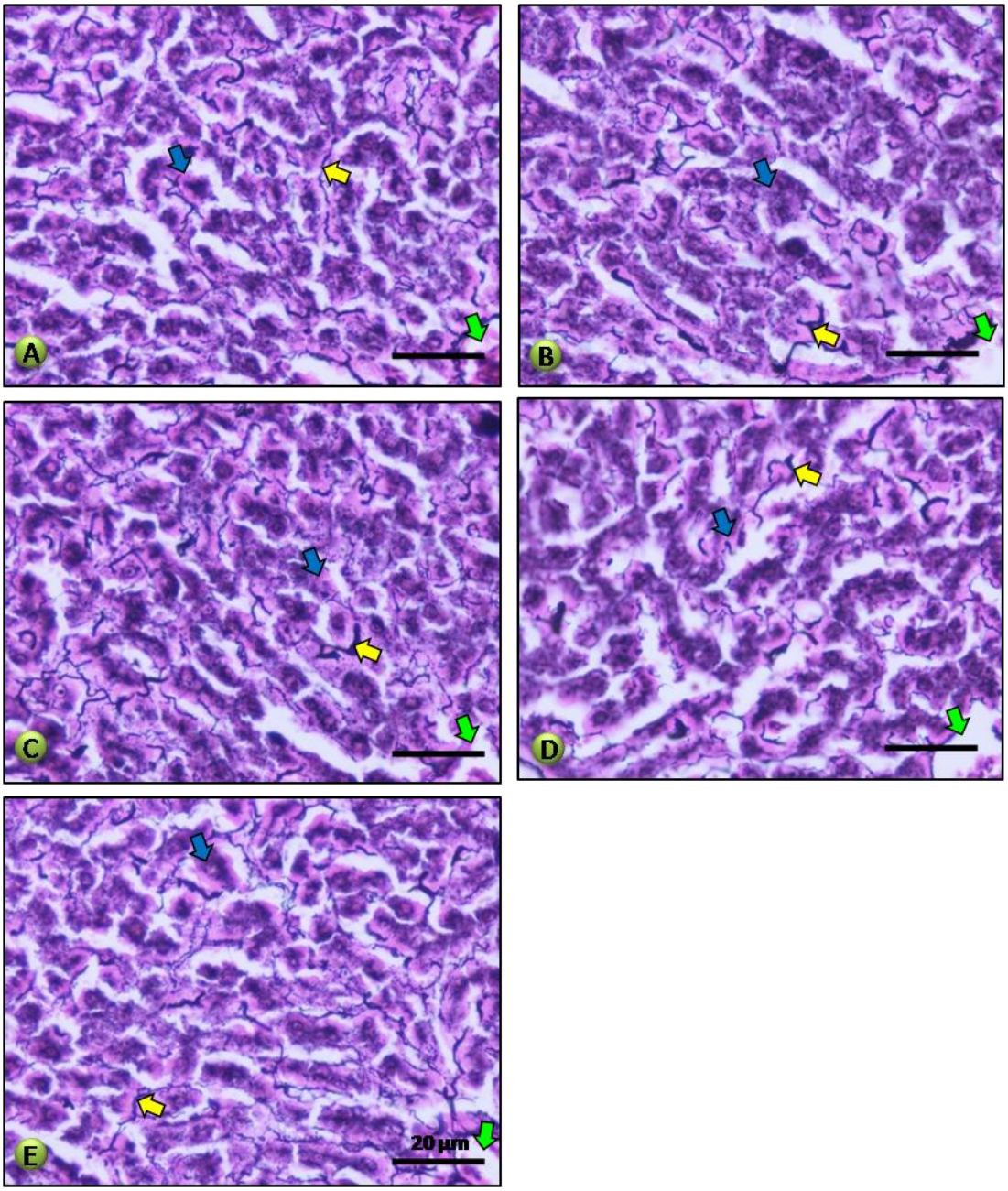

Figure 3. *Kh does not increases reticular fibers:* A-E) Control and experimental groups show normal reticular fibers, fibers (yellow arrow), contrast stain (blue arrow), central vein (green arrow). Wilder´s reticulin stain. Paraffin embedded, light microscopy. Bar: 20 µm.

with extended areas of necrotic hepatocytes and hepatocytes with large cytoplasmic vacuoles. In the samples of recovery group only vascular congestion and few and small cytoplasmic vacuoles were observed.

DISCUSSION

Since numerous reports of accidental intoxication in humans (Arellano et al., 1994; Bermúdez et al., 1995; Ocampo et al., 2007) or experimental intoxication in animals with *Kh* fruit (Escobar and Nieto, 1965; Charlton and Pierce, 1970; Muñóz and Chávez, 1979; Muñóz et al., 1983; Bermúdez et al., 1986; Bermúdez et al., 1992; Salazar et al., 2006, García-Juárez et al., 2012) were focused on the alterations of peripheral nerve, it was considered for a long time that *Kh* affects exclusively peripheral nerve system (PNS). However, this study is

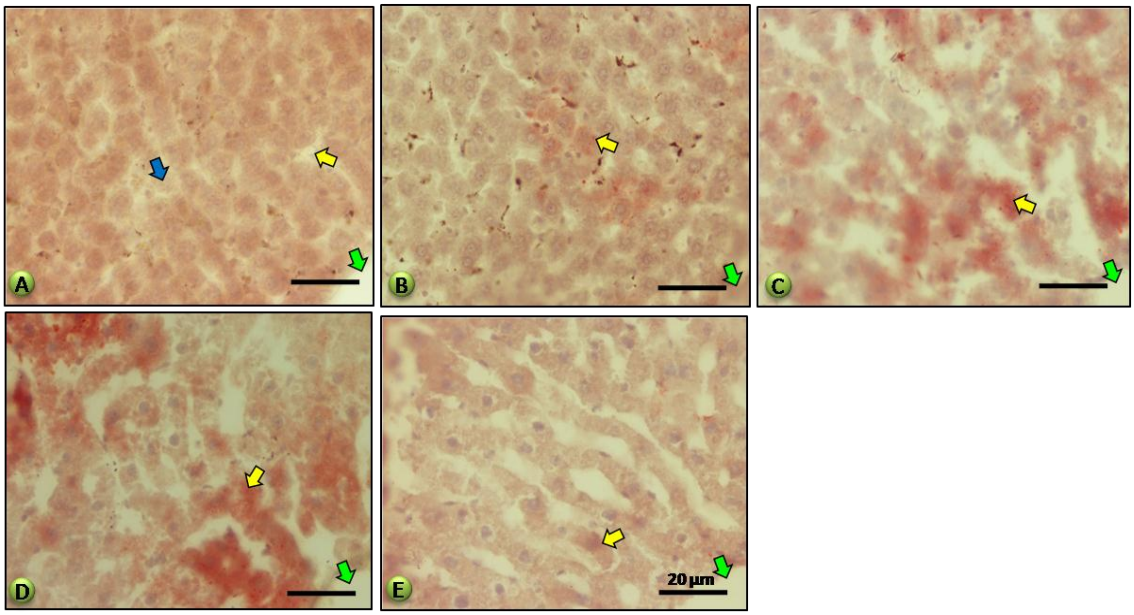

Figure 4. *Kh induces steatosis in intoxicated groups*: A) Control group with absence of lipids in the cytoplasm of hepatocytes (blue arrow), sinusoids (yellow arrow), central vein (green arrow). B-D) Groups without paresis, paresis and paralysis, respectively, showing increasing amount of lipids (yellow arrows), central vein (green arrows). E) Recovery group shows scarce lipids remaining (yellow arrow). Oil red histochemistry. Bar: 20 µm.

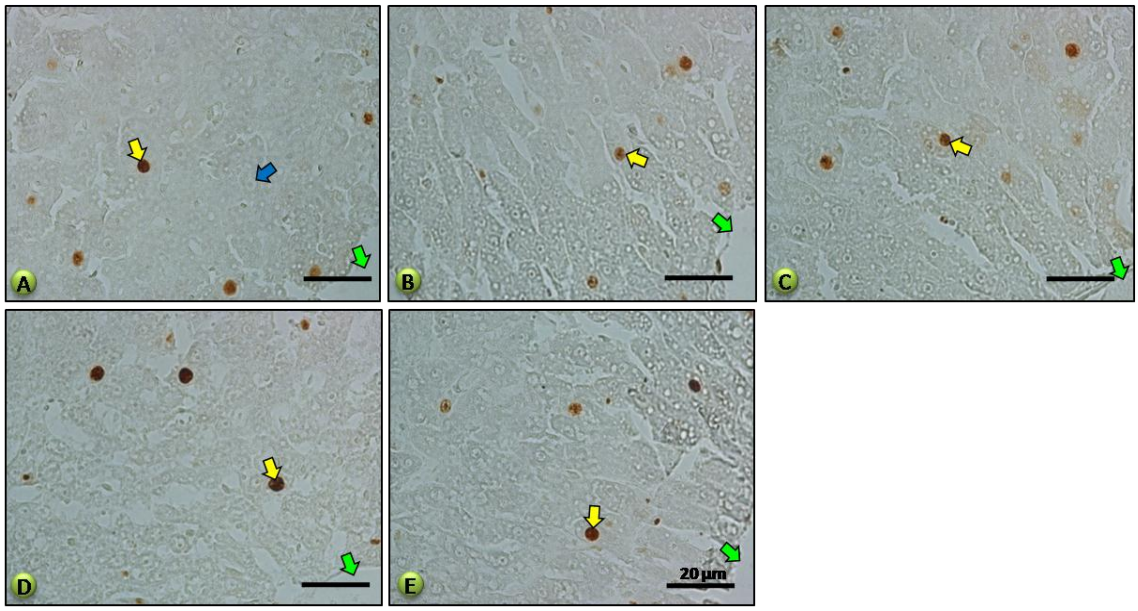

Figure 5. *Kh does not induce apoptosis in chronic intoxicated rats:* A-E) Control group and experimental groups showing scarce cells positive for chromatin fragmentation, positive nuclei (yellow arrow), negative nuclei (blue arrow), central vein (green arrow). TUNEL staining. Bar: 20 µm.

the first to describe the histopathological alterations in the liver caused by *Kh* fruit in an experimental model of peripheral neuropathy. These alterations began at 24 days post-intoxication and increased at 48 and 58 days post-intoxication, but at 112 days post-intoxication some alterations disappeared, demonstrating a possible recovery of liver. Previously we have described histopathological alterations in cerebral motor cortex,

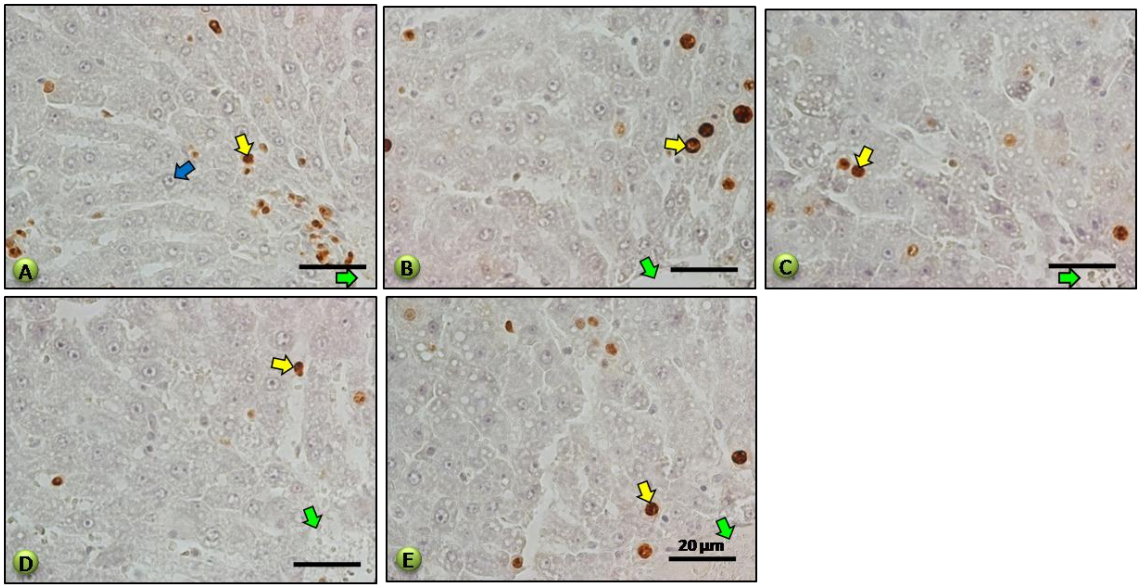

Figure 6. *Kh induces an antiproliferative effect:* A) Control group with numerous proliferation positive nuclei (yellow arrow), negative nuclei (blue arrow), central vein (green arrow). B-E) Intoxicated groups showing decreasing positive nuclei and an increase in the recovery group, central vein (green arrow). PCNA immunohistochemistry. Paraffin embedded, light microscopy. Bar: 20 µm.

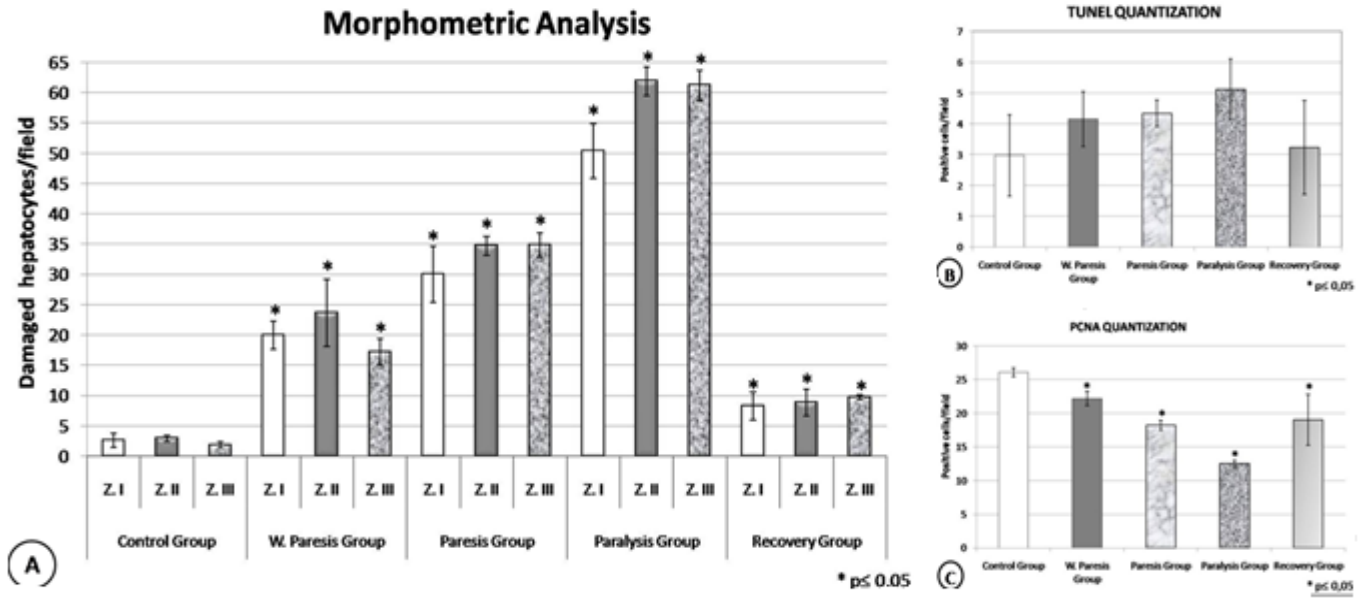

Figure 7. Morphometric analysis. A) number of damaged hepatocytes, showing increasing damage in liver cells in intoxicated groups and a decrease in recovery group. Intoxicated groups show statistically significant difference compared with control group. * p≤0,05. B) Number of positive nuclei to chromatin fragmentation with TUNEL method, no statistically significant difference was observed between control and intoxicated groups. * p≤0,05. C) Number of proliferating nuclei measured by PCNA immunohistochemistry, showing decreasing positive cells in intoxicated groups and an increase in recovery group. Intoxicated groups showed statistically significant difference compared with control group. * p≤0,05.

cerebellum, spinal cord, vestibular nucleus, and corticopontocerebellar tract (Becerra-Verdín et al., 2009) and recently in striatum (Díaz-Pérez et al., 2016); as well as severe damage in kidney and lung (García et al., 2013

a, b). Furthermore, the present investigation also contributes to the fact that accidental intoxication with *Kh* in humans and experimentally in animals causes a systemic damage in addition to the damage of PNS in this experimental model (Salazar et al., 2006).

Clinical manifestations, such as weight loss, ocular secretion, hair bristling, weakness, and respiratory difficulty, were analyzed in the rats intoxicated with *Kh* fruit. These manifestations were present in the paresis group at 48 days, were more evident at 58 days in the paralysis group, and almost all of the symptoms resolved in the recovery group, which only presented piloerection. These results agree with other studies regarding the clinical signs in humans and animals intoxicated with *Kh* fruit (Padron-Puyou, 1951; Padrón and Velázquez, 1956; Bermúdez et al., 1986; Salazar et al., 2006, García-Juárez et al., 2012).

In this study, we observed a gradual increase of necrotic hepatocytes with abundant vacuolated spaces, as well as vascular congestion and hemorrhagic signs in sinusoids in the groups intoxicated with *Kh* fruit. These signs agree with the findings reported by Bermúdez et al., (1986) who studied the effect of T-514, one of the toxins isolated from *Kh* fruit on liver.

The increasing areas of necrosis in the treated groups were observed in the morphometric analysis, showing the highest amount of necrotic cells in the paralysis group that decreased in the recovery group. This finding has not been described before for chronic intoxication with *Kh* fruit. It has been described that several plants as *Larrea tridentata* (Stickel et al., 2000), and *Ruta graveolens* (Serrano-Gallardo et al., 2013) can cause a hepatotoxic effect similar to the necrotic damage observed in this study.

Another important point is that even though experimental studies of acute intoxication in different animal species with isolated toxins or *Kh* fruit have reported similar alterations in liver to those observed in the present investigation (Bermúdez et al., 1986; 1992). These studies do not report the progression and recovery of the histopathological damage in the liver observed in the present investigation.

The liver necrosis observed in the present investigation correlates with other experiments reporting that acute administration of ground fruit of *Kh* causes a significant increase of transaminases AST and ALT levels in serum (Jaramillo et al., 2009), where the increase of these enzymes is indicative of hepatic necrosis.

An *in vitro* study using the toxin T-514 showed that it suppresses the metabolic activity of mitochondria and it induces the production of reactive oxygen species, both in primary cultures of hepatocytes and microsomes (Garza-Ocañas et al., 2003). Furthermore, an *in vitro* study performed by Wheeler et al., (1971) using ether extracts of *Kh* reported that the extracts decreased oxygen consumption, and they produced inhibitory effects. In the same study they observed an uncoupling effect of the respiration chain and an inhibition in the oxidative phosphorylation in mitochondria from rat liver (Wheeler et al., 1971). These alterations could be part of the mechanisms of hepatic cytotoxicity observed in the present investigation.

The recovery of liver necrosis observed in the recovery group at 112 days post-intoxication with *Kh*, correlates with the high capacity of regeneration of hepatocyte as it has been reported in experimental models treated with chemical agents, where the organ regenerates when the toxic stimulus is removed (Fausto et al., 2000). Moreover, the hepatic steatosis observed in treated groups in this study has not been reported previously in the chronic intoxication model with *Kh* fruit. The finding that it was reversible in the recovery group correlates with reported experimental intoxications with chemical agents where hepatic steatosis is a normal response to toxic stimuli, and it is a reversible injury when the stimulus is removed (Riet-Correa et al., 1986; Islas et al., 1991).

On the other hand, it has been proposed that steatosis is caused by an inhibition of the hepatic lipid transportation system (Fromenty et al., 1995; Jaeschke et al., 2002; Xu et al., 2003). These findings suggest that during the chronic intoxication with *Kh* there is induction of steatosis in the treated groups, but probably the toxic stimulus decreases or ends at the last stages allowing the reversal of hepatic steatosis observed in the recovery group.

In the present study, the areas of necrotic cells were analyzed with the TUNEL assay for chromatin fragmentation, one of the characteristics of apoptosis; and the results showed that few cells were positive in control and intoxicated groups, which demonstrated a normal turnover of hepatocytes. However, no significant difference in the number of positive cells was found among all groups. These results are different compared to findings described in liver of rats treated with *Ruta graveolens* where necrotic and apoptotic hepatocytes were detected in intoxicated groups (Serrano-Gallardo et al., 2013; Soto-Domínguez et al., 2013). In liver of CD-1 mouse intoxicated with 28 mg of PA1 (toxin T-514)/kg body weight, it was observed that apoptosis was extensive in liver samples (Soto-Domínguez, 2005), in contrast to the present investigation that demonstrated a necrotic effect of *Kh* fruit.

Using the specific monoclonal antibody anti-PCNA, we observed the largest number of positive cells in the control group; that gradually decreased in intoxicated groups and increased again in the recovery group. This was confirmed in the morphometric analysis. These results are similar to those observed in liver of rats treated with *Ruta graveolens* where this plant showed an antiproliferative effect in intoxicated groups (Serrano-Gallardo et al., 2013).

The observation of histopathological alterations in the liver of animals intoxicated with *Kh* fruit, contributes to the knowledge of the toxicological effect of this plant to

determine whether this intoxication also affects other organs besides the central and peripheral nervous system. Further studies will be required to elucidate the mechanism of damage and recovery in the hepatocytes observed in this study. Currently *in vitro* and *in vivo* studies, related to the aforementioned observations are being performed in the present investigation, as well as studies to evaluate the effect of toxins isolated from the *Kh* seed, such as T-514 administered at different durations and concentrations.

Conflict of Interests

The authors have not declared any conflict of interests.

ACKNOWLEDGMENTS

This study was supported by a grant from CONACYT for RGG. We acknowledge the work of QCB Rosa Maria Leal G. and Nora Frías Trejo for technical assistance involved in electron microscopy processing and ultramicrotomy, and to Stefanie Galue for reviewing English manuscript. Present study is dedicated to memory of Ph.D. Julio Sepúlveda-Saavedra (†February 10th, 2014) Chairman of Histology Department, Faculty of Medicine, UANL until the day of his death.

REFERENCES

Arellano CE, Mendoza CJ, Domínguez CF (1994). Intoxicación por *Karwinskia johnstonii*: Estudio de 12 pacientes. Bol. Med. Hosp. Infant. Mex. 51:105112. Available at: http://cat.inist.fr/?aModele=afficheN&cpsidt=3964264

.Becerra-Verdin EM, Bermúdez-Barba MV, Salazar-Leal ME, Ancer Rodríguez J, Romero-Diaz V, Soto-Domínguez A, Ballesteros-Eliozondo RG, Saucedo-Cardenas O, Piñeyro Lopez A, Sepúlveda-Saavedra J (2009). *Karwinskia humboldtiana* (buckthorn) fruit causes Central Nervous System damage during chronic intoxication in the rat. Toxicon 53(6):645-51.

Bermúdez MV, González-Spencer D, Guerrero M, Waksman N, Piñeyro A (1986). Experimental intoxication with fruit and purified toxins of Buckthom (*Karwinskia humboldtiana*). Toxicon 24:1091-1097.

Bermúdez MV, Lozano FE, Salazar ME, Waksman N, Piñeyro A. (1995). Intoxicación de una familia con *Karwinskia humboldtiana* (tullidora). Gac. Méd. Mex. 131:100-106.

Bermúdez MV, Martínez FJ, Salazar ME, Waksman N, Piñeyro A. (1992). An experimental acute intoxication with Ripe Fruir of *Karwinskia humboldtiana* (tullidora) in Rat, Guinea pig, Hamster and Dog. Toxicon 30:1493-1496.

Bustamante S, Olvera R, Correa N (1978). Intoxicación fatal por tullidora (*Karwinskia humboldtiana*). Gac. Méd.Mex. 4:241-244.

Castillo-Nájera F (1920). Contribución al estudio de la parálisis tóxica. Un envenenamiento colectivo con tullidora. En Memoria del V Congreso Médico. Dirección de Talleres Gráficos Méx. pp. 240-244.

Charlton KM, Pierce KR (1970). A Neuropathy in Goats Caused by Experimental Coyotillo (*Karwinskia-humboldtiana*). Poisoning Part V Lesions in the Central Nervous System. Pathol. Vet. 7:435-47.

Díaz-Pérez RN, Castillo-González JA, Carcaño-Díaz K, García-Juárez J, Salazar-Leal ME, Montes-de-Oca-Luna R, Saucedo-Cárdenas O and Soto Domínguez A (2016). Histopathological Alterations in Striatum Caused by *Karwinskia humboldtiana* (Buckthorn) Fruit in An Experimental Model of Peripheral Neuropathy. Histol. Histopathol. 31:393-402.

Dreyer DL, Arai I, Bachman CD, Anderson WR, Smith RG, Daves GD. (1975). Toxins Causing no inflammatory Paralytic Neuropathy Isolation and Structure Elucidation. J. Am. Chem. Soc. 97:4895-990.

Escobar A, Nieto D (1965). Aspectos neuropatológicos de la intoxicación con *Karwinskia humboldtiana.* Estudio experimental. Gac. Med. Mex. 95:163-177.

Fausto N (2000). Liver regeneration. J. Hepatol. 32:19-31.

Fernández R (1992). Nombres Comunes uso y distribución del genero *Karwinskia* (*Rhamnaceae*) en México. Anal. Inst. Biol. Univ. Auton Méx Set Bot. 63:1-23.

Fromenty B, Pessayre D (1995). Inhibition of mitochondrial beta-oxidation as a mechanism of hepatotoxicity. Pharmacol. Ther. 67(1):101-154.

García R, Salazar ME, Becerra EM, Romero V, García J, Soto A, Sepúlveda J (2013a). Lung and Peripheral Nerve Mast Cells in Chronic Intoxication with *Karwinskia humboldtiana* in Wistar Rat: Histological and Histochemical Studies. Int. J. Morphol. 31(4):1216-1222.

García GR, Salazar LME, Romero DV, García JJ, Soto DA, Juárez ROA, Sepúlveda SJ (2013b). Chronic Intoxication with Ripe Fruit of *Karwinskia humboldtiana* in Wistar Rats: Renal Damage. Int. J. Morphol. 31(4):1449-1454.

García-Juárez J, Salazar-Leal ME, Guzmán-López S, Romero-Díaz VJ, Ramírez-Durón R, Sepúlveda-Saavedra J (2012). Evaluation of the Effect of Treatment with Lipoic Acid Administered to the Wistar Rat Intoxicated with the Fruit of *Karwinskia humboldtiana*. Int. J. Morphol. 30 (2):572-578.

Garza-Ocañas L, Zanatta-Calderón MT, Acosta A, Torres-Alanís O, Piñeyro-López A (2003). Production of reactive oxygen species by toxin T-514 of genus *Karwinskia in vitro*. Toxicol. *in vitro*. 17(1):19-25.

Gavrieli Y, Sherman Y, Ben-Sasson SA (1992). Identification of programmed cell death *in situ* via specific labeling of nuclear DNA fragmentation. J. Cell Biol. 119(3):493-501.

Islas A (1991). Intoxicación con palqui (*Cestrumparqui*) en bovinos. Pat Anim. 5(1):32-33.

Ito S, Karnowsky M (1968). Formaldehyde-glutaraldehyde fixative containing trinitro compounds. J. Cell Biol. 39:168a-9a.

Jaeschke H, Gores GJ, Cederbaum AI, Hinson JA, Pessayre D, Lemasters JJ. (2002). Mechanisms of Hepatotoxicity. Toxicol. Sci. 65(2):166-176.

Jaramillo J, Rodríguez V, Castillo C, Quezada T, Cerda G, Posadas F, Taboada C (2009). Daño hepático y en la coagulación de la sangre producido por la administración de los frutos maduros de la planta tullidora (*Karwinskia humboldtiana*) en la rata. Rev. Mex. Cienc. Farm. 40(1):28-34.

Matsumoto K, Moriuchi T, Koji T, Nakane PK (1987). Molecular cloning of cDNA coding for rat proliferating cell nuclear antigen (PCNA)/cyclin. EMBO J. 6(3):637-42.

Muñóz ME, Chávez B (1979). Conduction block and functional denervation caused by tullidora (*Karwinskia humboldtiana*). Exp. Neurol. 65:255-270.

Muñóz ME, Chávez B, Nathan J (1983). Denervation caused by tullidora (*Karwinskia humboldtiana*). Neuropathol. Appl. 9(2):121-134.

Ocampo RL, Ontiveros NO, Fernández LO (2007). Intoxication with buckthorn (*Karwinskia humboldtiana*): report of three siblings. Pediatr. Dev. Pathol. 10:66-68.

Padron-Puyou F (1951). Clinical and experimental studies on paralysis in children due to *Karwinskia humboldtiana*. Gac. Med. Mex. 81(2-4):299-311.

Padrón F, Velázquez T (1956). Patología experimental y clínica de la parálisis por *Karwinskia humboldtiana*. Rev. Mex. Ped. 25:225-237.

Puértolas MM, Nava JO, Medina LH, López OF, Oyervides PJ (1984). Polirradiculoneuritis por *Karwinskia humboldtiana*. Informe de seis casos. Rev. Med. IMSS. (Mex). 22:22-27.

Riet-Correa F, Schield AL, Méndez MC, Pinheiro MH (1986). Intoxicaçào por *Cestrumparqui* (*Solanaceae*) em bovinos no Río Grande do Sul. Pesq. Vet. Bras. 6:111-115.

Rivas V, Torres R, Waksman N (1990). Dimeric anthracenones from *Karwinskia* species. J. Med. Plant Res. 56(6):562-564.

Secretaría de Agricultura, Ganadería, Desarrollo Rural, Pesca y Alimentación (SAGARPA) (1999). Norma Oficial Mexicana NOM-062-

ZOO-1999, Especificaciones técnicas para la producción, cuidado y uso de los animales de laboratorio.

Salazar-Leal ME, Flores MS, Sepúlveda-Saavedra J, Romero-Díaz VJ, Becerra-Verdín EM, Taméz-Rodrìguez VA, Martínez HR, Piñeyro-López A, Bermúdez MV (2006). An experimental model of peripheral neuropathy induced in rats by *Karwinskia humboldtiana* (buckthorn) fruit. J. Peripher. Nerv. Syst. 11(3):253-61.

Segovia PA, Zermeño F (1972). Polirradiculoneuritis tóxica por *Karwinskia humboldtiana.*A propósito de un caso. Biol. Med. Hosp. Infant. 29:98-90.

Sepúlveda-Saavedra J, González-Corona B, Taméz-Rodríguez VA, Bermúdez MV, Piñeyro A (1992). Ultrastructure of the lesion induced by toxin T-514 isolated from *K. humboltiana* in the alveolar region of the lung. Proc. 50th Ann. Meet. EMSA. Bailey GW, Bentley J, Small JA (Eds). Published by San Francisco press, Inc. pp. 640-641.

Serrano-Gallardo LB, Soto-Domínguez A, Ruiz-Flores P, Nava-Hernández MP, Morán-Martínez J, García-Garza R, Martínez-Pérez EF (2103). Toxic Effect of Aqueous Extract of *Ruta graveolens* from the North of Mexico on the Liver of Wistar Rat. Int. J. Morphol. 31(3):1041-1048.

Soto-Domínguez A (2005). Evaluación morfológica y bioquímica de la presencia de apoptosis en varios órganos del ratón tratado con una dosis tóxica de Peroxisomicina A1, 2005. Tesis de Maestría. Facultad de Medicina. UANL.

Soto-Domínguez A, Serrano-Gallardo LB, García-Garza R, Ruíz Flores P, Morán-Martínez J, Nava-Hernández MP, Martínez-Pérez EF (2013). Aqueous Extract of *Ruta graveolens* From the North of Mexico Causes Apoptosis and Shows Antiproliferative Effect on the Liver of Wistar Rat: Morphological Evidence. Int. J. Morphol. 31(4):1340-1348.

Stickel F, Egerer G, Seitz H (2000). Hepatotoxicity of botanicals. Public Health Nutr. 3:113-124.

Wheeler MH, Camp BJ (1971). Inhibitory and uncoupling actions of extracts from *Karwinskia humboldtiana* on respiration and oxidative phosphorylation. Life Sci. 10(1):41-51.

Waksman N, Martínez L, Fernández R (1989). Chemical and toxicological screening in genus *Karwinskia*. Rev. Latinoamer. Quim. 20(1):27-29.

Waksman N, Ramirez R (1992). Isolation of a new dymeric anthracenone from *Karwinskia parvifolia*. Rev. Latinoamer. Quim. 23(1):25-27.

Xu A, Wang Y, Keshaw H, Xu LY, Lam KSL, Cooper GJS (2003). The fat-derived hormone adiponectin alleviates alcoholic and nonalcoholic fatty liver diseases in mice. J. Clin. Inv. 112(1):91-100.

Zhang G, Gibbs E, Kelman Z, O'Donnell M, Hurwitz J (1999). Studies on the interactions between human replication factor C and human proliferating cell nuclear antigen. Proc. Natl. Acad. Sci. U.S.A. 96(5):1869-74.

academicJournals

Vol. 10(26), pp. 390-401, 10 July, 2016
DOI: 10.5897/JMPR2016.6162
Article Number: B1CF05959540
ISSN 1996-0875

http://www.academicjournals.org/JMPR

Journal of Medicinal Plants Research

Full Length Research Paper

Characterization of the bioactive constituents of *Nymphaea alba* rhizomes and evaluation of anti-biofilm as well as antioxidant and cytotoxic properties

Riham Omar Bakr[1]*, Reham Wasfi[2], Noha Swilam[3] and Ibrahim Ezz Sallam[1]

[1]Pharmacognosy Department, October University for Modern Sciences and Arts (MSA), Giza, Egypt.
[2]Microbiology and Immunology Department, Faculty of Pharmacy, October University for Modern Sciences and Arts (MSA), Giza, Egypt.
[3]Pharmacognosy Department, Faculty of Pharmacy, British University in Egypt (BUE), Cairo, Egypt.

Received 29 May, 2016; Accepted 5 July, 2016

Anti-biofilm represents an urge to face drug resistance. *Nymphaea alba* L. flowers and rhizomes have been traditionally used in Ayurvedic medicine for dyspepsia, enteritis, diarrhea and as an antiseptic. This study was designed to identify the main constituents of *Nymphaea alba* L. rhizomes and their anti-biofilm activity. 70% aqueous ethanolic extract (AEE) of *N. alba* rhizomes was analyzed by liquid chromatography, high resolution, mass spectrometry (LC-HRMS) for its phytoconstituents in the positive and negative modes in addition to column chromatographic separation. Sixty-four phenolic compounds were identified for the first time in *N. alba* rhizomes. Hydrolysable tannins represent the majority with identification of galloyl hexoside derivative, hexahydroxydiphenic (HHDP) derivatives, glycosylated phenolic acids and glycosylated flavonoids. Five phenolics have been isolated and identified as gallic acid and its methyl and ethyl ester in addition to ellagic acid and pentagalloyl glucose. Minimum inhibitory concentrations (MIC) and anti-biofilm activity for the extract and the major isolated compounds were determined. Radical scavenging activity using 2.2Di (4-tert-octylphenyl)-1-picryl-hydrazyl (DPPH) assay as well as cytotoxic activity using 3-(4, 5-dimethyl thiazol-2-yl)-2, 5-diphenyl tetrazolium bromide (MTT) assay have also been evaluated. MIC of *N. alba* rhizomes against *Staphylococcus aureus* was 0.25 mg/mL compared with 0.1 mg/mL for methyl gallate. The best reduction in biofilm formation (84.9%) as well as the best radical scavenging (IC_{50} 3 µg/mL) and cytotoxic (IC_{50} 9.61 ± 0.3 µg/mL) activities were observed with methyl gallate. This is the first study for in-depth characterization of phenolic compounds in *N. alba* rhizomes revealing it as a valuable source of phenolic compounds and promising anti-biofilm forming agent of natural origin.

Key words: Hydrolysable tannins, Nymphaeaceae, LC-HRMS.

INTRODUCTION

Bacterial illnesses are caused by many virulence factors. Biofilm forming capacity is an additional virulence factor

*Corresponding author. E-mail: rehambkr@yahoo.com, romar@msa.eun.eg. Tel: (202)-01006516956.

that assists the persistence of pathogens in harsh environmental conditions (Upadhyay et al., 2014). Cells in biofilms grow as communities, surrounded by a self-produced thick layer of extracellular polymeric substances (EPS, also known as matrix or slime) (Sauer and Camper, 2001). The extracellular matrix of biofilm-embedded microorganisms is capable of sequestering and concentrating environmental nutrients such as carbon, nitrogen and phosphate. In addition, they can evade multiple clearance mechanisms produced by host and synthetic sources such as antimicrobial and anti-fouling agents, shear stress, host phagocytic elimination and host radical and protease defenses (Archer et al., 2011).

Anti-biofilms have attracted the attention of scientists for the last forty years to combat biofilms that are involved in a wide range of infections and antibiotic-resistant infections, in a trial to develop new and effective antimicrobial agent with high efficiency.

Gram-positive bacteria are the commonest cause of nosocomial infections with predominance of *Staphylococcus aureus* (Valentino et al., 2014). *Staphylococcus* is the most common infectious agent in skin, mucous commensal and indwelling medical devices (Otto, 2009). *S. aureus* biofilm-associated infections are difficult to treat with antibiotics and devices need to be replaced more frequently than those infected with *Staphylococcus epidermidis* (Jones et al., 2001).

Traditional medicine attracted the attention of traditional healers and scientists thousands of years ago. World Health Organization (WHO) estimated that about three-quarters of the world population living in developing countries relied upon traditional remedies (mainly herbs) for the health care of its people (Gilani and Rahman, 2005).

Tannins are polyphenolic compounds with wide range of biological activities. The mode of antimicrobial action of tannins is potentially due to the inactivation of microbial adhesins and cell envelope transport proteins (Saura-Calixto and Pérez-Jiménez, 2009).

Nymphaea alba L. (Nymphaeaceae), also known as the European White Waterlily, White Lotus or Nenuphar, is an aquatic flowering plant with perennial rhizomes or rootstocks anchored with mud (Wiersema, 1987). There are approximately 50 species in this genus. The flowers are white and they have many small stamens inside. Water-lilies have extensive rhizome systems from which leaf and flower stalks emerge each year. The root of the plant was used by monks and nuns for hundreds of years as an aphrodisiac, being crushed and mixed with wine. The dried roots and rhizomes of the white water lily have been used orally to treat gastrointestinal, genital, and bronchial conditions (Khan and Sultana, 2005). Interest on rhizomes of *N. alba* has increased. Bose et al. (2013) proved its possible sedative as well as powerful uterotonic effects (Bose, 2014). Moderate antioxidant activity, analgesic and anti-diarrheal activities have been also proved (Bose, 2012a, b). Although of promising results, to the best of our knowledge, no scientific reports have been found concerning chemical characterization of rhizomes as well as its antimicrobial activity. Therefore, the aim of this study was to get in-depth identification of phenolic constituents of *N. alba* rhizome extract using LC-MS and X calibur software, in addition to the isolation of its main constituents and evaluation of their antimicrobial as well as cytotoxic activities.

MATERIALS AND METHODS

General experimental procedures

For column chromatography, microcrystalline cellulose (E. Merck, Darmstadt, Germany) and Sephadex LH-20 (Pharmacia, Uppsala, Sweden) were used. For paper chromatography; Whatman no. 1 sheets, Whatman no. 3 sheets (for Preparative Paper Chromatography, PPC) (Whatman Ltd, Maidstone, Kent, England) were used. The pure compounds were visualized under UV light (254 and 365 nm) with exposure to NH_3 vapor or spraying with $FeCl_3$ (1% in ethanol). Solvent systems S_1 (*n*- BuOH/HOAc/H_2O; 4:1:5 v/v/v top layer), and S_2 (15% aqueous HOAc) were used. The NMR spectra were recorded at 300 (^1H) and 75 (^{13}C) MHz on a Varian Mercury 300. The results were reported as δ ppm values relative to TMS in the convenient solvents. UV analysis for pure samples was recorded on MeOH solutions and with different diagnostic UV shift reagents on a Shimadzu UV spectrophotometer (1800 UV probe). LC-HRESI-MS-MS was performed on a Bruker micro-TOF-Q Daltonics (API) Time-of-Flight mass spectrometer (Bremen, Germany), coupled to 1200 series HPLC system (Agilent Technologies, Waldbronn, Germany), equipped with a high performance autosampler, binary pump, and PDA detector G 1314 C (SL). Chromatographic separation was performed on a Superspher 100 RP-18 (75 × 4 mm i.d.; 4 μm) column (Merck, Darmstadt, Germany).

Preparation of plant extract

Rhizomes of *N. alba* L. were collected from AL Orman garden, Giza, Egypt in November 2012 during the flowering stage. Authentication of the plant was performed by *Dr*. Therese Labib Youssef (consultant of plant taxonomy, Ministry of Agriculture). A voucher specimen (RS006) was deposited at the herbarium of the Pharmacognosy Department, Faculty of Pharmacy, October University for Modern Science and Arts (MSA), Egypt.

N. alba rhizome (300 g) was dried, reduced, and sieved to obtain the powdered rhizome, extracted with 70% ethanol under reflux. The aqueous ethanolic extract (AEE) was filtered, concentrated using a rotary evaporator and dried in vacuum at 40°C, to yield 40 g (13.3% yield).

Identification of phenolic compounds of aqueous ethanol extract of *N. alba* rhizomes by LC-HRMS

N. alba AEE was investigated according to Hassaan et al. (2014). The mobile phase consisted of (A) 2% acetic acid (pH 2.6) and (B) 80% methanol. Gradient elution at a flow rate of 100 μL/min was used from 5 to 50% B at 30°C. Pneumatically assisted electrospray ionization was used. Spectra were recorded in positive and negative ion mode between m/z 120 and 1,500 with 4000V capillary voltage. Heated dry nitrogen gas at temperature 200°C and flow rate 10 L/min was used. The gas flow to the nebulizer was set at pressure 1.6 bar. For collision-induced dissociation (CID) MS-MS

measurements, the voltage over the collision cell varied from 20 to 70 eV and Argon was used as collision gas. Data analysis software was used for data interpretation. Sodium formate was used for calibration at the end of LC-MS run. Interpretation for ESI-MS was performed by Xcalibur 2.1 software from Thermo Scientific (Berlin, Germany).

Total phenolic and flavonoid content

The total phenolic content (TPC) was determined using the Folin-Ciocalteu's reagent. Concentration of phenolic content was expressed as gallic acid equivalent (GAE) (Sellappan and Akoh, 2002). Flavonoid content (FC) was estimated using aluminum chloride colorimetric assay. Concentration of flavonoid content was expressed as quercetin equivalent (QE) (Kosalec et al., 2004).

Extraction and isolation

AEE (25 g) was fractionated on a cellulose column (375 g, 110 × 7 cm) using a step-gradient from 10% MeOH in H_2O to 100% MeOH, to yield 80 fractions of 100 mL each, which were further collected into 5 major collective fractions (I-IV) monitored using paper chromatography and solvents S_1 and S_2 visualized using UV-light. Fraction I (2.55 g) was found to be polyphenolic-free ($FeCl_3$ spray reagent/PC). Fraction II (10% MeOH, 1.5 g) was applied on Sephadex LH-20 eluted with 50% methanol to afford **1** (15 mg each). Fraction III (70% MeOH, 400 mg) was chromatographed on PPC using S1 as solvent followed by further purification using Sephadex LH-20 affording **2** and **3**. Fraction IV (100% MeOH, 2.5 g) was chromatographed on a microcrystalline cellulose column using saturated butanol as a solvent then further purified on Sephadex LH-20 affording **4** and **5.** All separation processes were followed up by Comp-PC with S_1 and S_2 solvents.

Bacterial and mycotic strains and growth conditions

Standard strains of *Bacillus subtilis (*ATCC 6633), *Sarcina lutea* (ATCC 9341), *Proteus vulgaris* (ATCC 6899), *Salmonella typhimurium* (ATCC 13311), *Shigella sonnei* (ATCC 9290), *Staphylococcus aureus* (ATCC 6538), *Escherichia coli* (ATCC 8739), *Pseudomonas aeruginosa* (ATCC 27853) and *Candida albicans* (ATCC 10231). In addition to four multi-drug resistant clinical isolates of *S.aureus* from wound infection (identified by microscopic, macroscopic and biochemical tests) (Cheesbrough, 2005).

Determination of microbial sensitivity to *N. alba* rhizome extract by disk diffusion method

Bacteria and *Candida albicans* were grown in nutrient broth and Sabarouds' dextrose broth, respectively, overnight and adjusted to a concentration of 10^8 CFU/mL by comparing it with McFarland standard 0.5.

For the disk diffusion assay, 1 mL of each bacterial suspension was uniformly spread on a solid growth medium in a Petri-dish. Four sterile paper disks (6 mm in diameter; Becton, Dickinson & Co.) were placed on the surface of each agar plate and were impregnated with 10 µL of the diluted plant extract (250 mg/mL). Plates were incubated for 24 h under appropriate cultivation conditions. Antimicrobial activity was measured as a diameter of inhibition zone around a disk following the 24 h incubation. Susceptibility was estimated by measuring the inhibition zone according to Valgas et al. (2007). Inhibition zones of 16-21 mm indicates strong activity, 12-16 mm denotes good activity, while 10-11 mm and <10 mm indicate intermediate and no activity, respectively. Disks impregnated with sterile distilled water and ethanol served as negative controls and a disk with an antibiotic (ofloxacin or Amphotericin B, Sigma-Aldrich GmbH, Steinheim, Germany) served as a positive control. Replicas at each concentration were performed.

Determination of minimum inhibitory concentrations (MIC) of *N. alba* rhizome extract and main constituents by microbroth dilution method

MIC was determined according to Klancnik et al. (2010), MIC of each antimicrobial was performed in flat-bottomed 96-well microplates (Greiner Bio-one, Stuttgart, Germany). This test was carried against standard strains of *B. subtilis (*ATCC 6633), *S. aureus* (ATCC 6538), *E. coli* (ATCC 8739), *P. aeruginosa* (ATCC 27853) and *C. albicans* (ATCC 10231). The antimicrobial activity of *N. alba* rhizome extract against standard *Staphylococcus aureus* was further confirmed by testing its activity against four clinical isolates of *S. aureus* (staph1-4). These clinical isolates were recovered from wound infection. To determine MIC of each, plant extract, and isolated compounds, dilution range was prepared one step higher than the final dilution range required from 0.15 to 2 mg/mL in Müeller Hinton broth.

The inoculum was prepared by adjusting the turbidity from an overnight microbial culture by comparing it to McFarland 0.5 and then diluting it to reach a final concentration of 10^6 CFU/mL. A volume of 75 µL of inoculum was added to equivalent volumes of the two-fold serially diluted plant extract or isolated compound in a microplate. Control wells were prepared with culture medium, bacterial suspension only, plant extracts only and ethanol in amounts corresponding to the highest quantity present. The plate was incubated for 24 h at 37°C and the MIC was recorded as the lowest concentration of antimicrobial which gave no visible growth. The average value of three replicates was taken.

Effect of *N. alba* rhizome extract and main constituents on bacterial biofilm

Strains, which showed sensitivity for antimicrobials of 1 mg/mL for extract were used in the next experiments as this might show promising activity (Rios and Recio, 2005). The effect of *N. alba* rhizome extract and its main constituents was evaluated on biofilm synthesis and the percentage reduction of biofilm was estimated. The concentration used was the MIC value for the plant extract and plant constituents against each isolate. This test was done by adding tested product, in desired concentration, after distribution of bacterial inoculum in microplate wells so that final concentration of bacteria was 5×10^5 cell/mL. The plates were incubated for 24 h at 37°C. The plates were then aspirated, washed, fixed and stained with crystal violet as described by Peeters et al. (2008). Readings of optical density at 545 nm, using microplate plate reader (Stat Fax®2100), in the presence of different concentrations of antimicrobials was compared to the positive control wells without antimicrobials (Yassien and Khardori, 2004).

$$\text{Percent reduction in biofilm formation} = \frac{A_c - A_t}{A_c} \times 100$$

Where Ac is OD_{545nm} for positive control wells and A_t is OD_{545nm} for biofilm in the presence of antimicrobials.

Radical scavenging activity

The activity of 1, 1-diphenylpicrylhydrazil (DPPH) was estimated

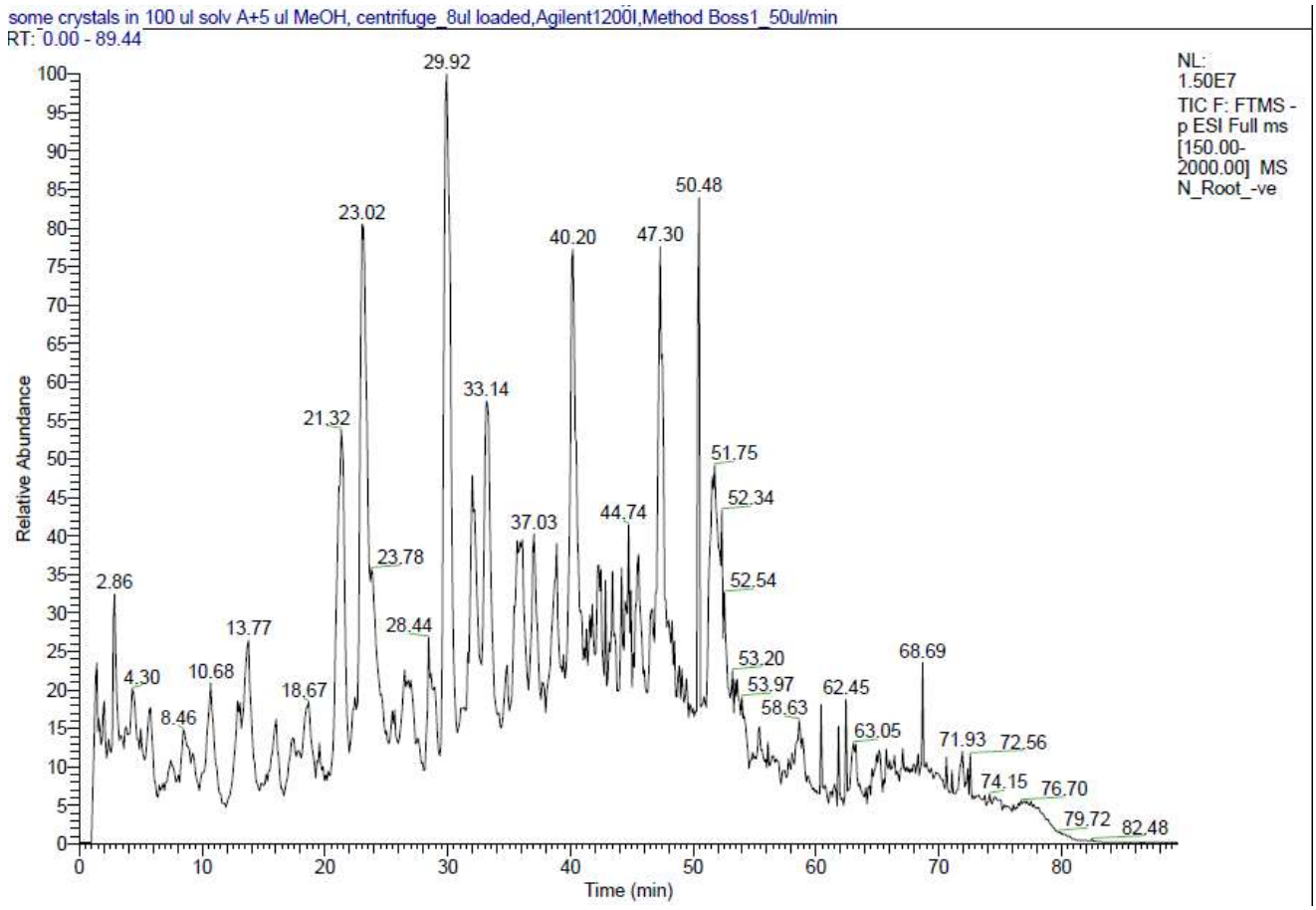

Figure 1. HPLC chromatogram of *N. alba* rhizomes.

according to the method described by Shimada et al. (1992). Radical scavenging activity was measured at 517 nm.

DPPH scavenging effect (%) = [(A0 - A1) / A0) × 100]

Where: A0 is the absorbance of the control reaction (DPPH) and A1 is the absorbance of the test extract. Ascorbic acid was used as standard (Oktay et al., 2003).

Cytotoxic activity

The viability of control and treated cells were evaluated at the Regional Center for Mycology and Biotechnology (RCMB) at Al-Azhar University using the MTT assay in triplicate. Liver carcinoma cell line (HepG2) was used to test the cytotoxic activity according to Fotakis and Timbrell (2006). Doxorubicin was used as the positive control drug while the untreated cells whose absorbance was considered as 100% represented the negative control. Serial two-fold dilutions of the tested compound and reference compound were estimated. The results were determined by three independent experiments (Wilson, 2000). Percentage cell viability was calculated as follows:

% Cell viability = (Mean Abs control – Mean Abs test metabolite) × 100/Mean Abs control

Where: Abs is absorbance at 570 nm.

The graphic plots were used for estimation of the 50% inhibitory concentration (IC_{50}). STATA statistical analysis package was used for the dose response curve drawing in order to calculate IC_{50}.

RESULTS AND DISCUSSION

As part of ongoing effort to investigate plants from traditional medicine, *N. alba* represents an interesting field of study where the rhizomes have not been previously studied and preliminary testing of flavonoid and phenolic contents showed high concentration, reflecting probably promising biological activities.

Phytochemical investigation

The TPC of *N. alba* AEE was estimated as 32.96 ± 0.86 mg/g GAE (standard curve equation: y = 0.0011x+ 0.0009, r2 = 0.9867) while the FC was evaluated as 0.43 ± 0.59 mg/g QE (standard curve equation: y = 0.005x-0.0198, r^2 = 0.9774). The considerable high phenolic and moderate flavonoid contents have a great impact on biological activities.

LC-HRMS

HPLC-MS-MS provides a powerful tool for phytochemical analysis in crude plant extracts. It provides useful structural information and allows for tentative compound identification when standard reference compounds are unavailable (Seeram et al., 2006). HPLC-MS-MS analysis of AEE of *N. alba* rhizomes revealed the identification of sixty-four phenolic compounds reported for the first time (Figure 1 and Table 1).

Identified compounds include, caffeic acid hexoside, syringic acid hexoside, p-coumaroyl quinic acid and protocatechuic acid. Hydrolysable tannins including, gallotannins and ellagitannins, in addition to epicatechin, flavone and flavonol aglycone and glycosides have also been identified (Table 1).

The main fragmentation pattern from gallotannins involved the loss of one or more galloyl groups (152 amu) and/or gallic acid (170 amu) from the deprotonated molecule $[M-H]^-$. However, the fragmentation pattern of ellagitannins was less clear than that of gallotannins as ellagitannins display enormous structural variability because of different linkages of HHDP residues with the glucose molecule and their strong tendency to form C-C and C-O-C linkages (Khanbabaee and Vanree, 2001).

Gallic acid (Pk **33**) was tentatively identified with [M-H] at m/z 169.01 and a characteristic daughter ion at m/z 125.06. While ellagic acid was identified with a precursor ion peak at [M-H] at m/z 301 and characteristic fragments at m/z 257, 229 and 185.

Digalloyl hexoside (pk **4**, [M-H] at m/z 483.08), trigalloyl (pk **21**, [M-H] at m/z 635.09), tetragalloyl (pk **42**, [M-H] at m/z 787.1), pentagalloyl (pk **17**, [M-H] at m/z at 939.02), hexagalloyl (Pk **59**, M-H at m/z 1091.12), as well as heptagalloyl (pk **43**, [M-H] at 1243.1) hexose were tentatively identified by sequential losses of galloyl moieties and appearance of daughter ion peaks at m/z 169 and 125 in addition to comparison with literature.

Pk **1** was tentatively identified as HHDP hexoside with a precursor ion at [M-H] at m/z 481.06 and daughter ions at m/z 301.12 and 275.16. Pk **8** was tentatively identified as galloyl HHDP-hexose with [M-H] at 633.07 and daughter ion at m/z 463.19 [M-H-170] and 301.13 [M-H-170-162]. Isomer with same molecular weight appeared at Pk **13** with different fragmentation pattern and daughter ion at m/z 451.12 and identified as isostrictinin (Galloyl HHDP hexose). The presence of a compound with the same molecular weight at different retention times illustrated one of its isomeric forms. Different isomeric forms of hydrolysable tannins were observed and have been reported previously in eucalyptus (Barry et al., 2001).

Pk **7** was tentatively identified as digalloyl HHDP-hexose (pedunculagin II) with [M-H] at m/z 785.11 and daughter ion at m/z 633.29 [M-H-152], 481.19 [M-H-152-152], 301.13 [HHDP]. Isomer appeared at Pk **38** with [M-H] at m/z 785.08 and daughter ion at m/z 483.28 [M-H-HHDP], 633.28 [M-H-152], 615.05 [M-H-152-H_2O] and base peak at m/z 301.11 was tentatively identified as tellimagrandin I isomer. Pk **51** was tentatively identified as trigalloyl HHDP hexose (tellimagrandin II) with a precursor ion at m/z 937.09 and daughter ion at 633.22 [M-H-digalloyl], 785.18 [M-H-152] and 301.15. Pk **46** with a precursor ion peak at 935.08 [M-H] was tentatively identified as casuarinin or galloyl–bis-HHDP-hexose, with daughter ions at m/z 633.23 [M-H-HHDP] and 301.14.

Flavonoids have been also tentatively identified as myricetin hexoside (Pk **6**) with [M-H] at m/z 479.05 and characteristic peak at 317.17; its pentoside (Pk **10**) with a precursor ion at m/z 449.04, while the aglycone was observed at Pk **52** with typical fragmentation pattern (Table 1). Quercetin pentoside (Pk **47**) was tentatively identified with [M-H] at m/z 433.04 while Pk **50** with [M-H] at m/z 463.05 and daughter ions at 343.16 [M-H-120], 373.17 [M-H-90] and characteristic base peak 301.15 was tentatively identified as quercetin hexoside. Kaempferol (Pk **53**) was identified with its hexoside derivative (Pk **58**). Pk **52** was tentatively identified as kaempferol glucuronide hexoside with m/z 623.13 [M-H], base peak 285.17 and daughter ion at 447.29 [M-H-176]. Apigenin (Pk **56**) and its glycosylated derivative have been also identified (Pk **57**, Pk **64**).

Isolated compounds

The 2D-PC screening of the AEE of *N. alba* rhizomes revealed the presence of phenolic compounds (color properties under UV-light and responses to NH_3). The isolated compounds were identified on the basis of their spectral data (UV, 1D NMR), co-chromatography, in addition to comparison with published references of phenolics or in family Nymphaeaceae, genus Nymphaea and *N. alba* flowers (Nonaka et al., 1987; Jambor and Skrzypczak, 1991; Nawwar et al., 1994; Li et al., 1999; Elegami et al., 2003). This study is the first report for isolation of phenolics from *N. alba* rhizomes.

Five main phenolics have been isolated and identified including, gallic acid and its methyl and ethyl ester, ellagic acid and pentagalloyl glucose. Methyl and ethyl gallate as well as pentagalloyl glucose, were tested for the differences in their response for antibiofilm, radical scavenging and cytotoxic activities.

1, 2, 3, 4, 6 Penta-O- galloyl β-D-glucose (1), failed to crystallize and was obtained as off-white amorphous powder. It gave violet blue color using short UV light and intense blue color with $FeCl_3$. UV λ_{max} (nm): 272 nm.^{1}H-NMR (300 MHz, DMSO-d_6): δ ppm 6.89, 6.84, 6.83, 6.82, 6.78 (each 2H, *s*, galloyl H-2 & H-6), 6. 32 (1H, *d*, J=8 Hz, glc, anomeric H-1), ^{13}C (75MHz, DMSO-d6): δ-ppm 165.29, 165.2, 164 (-COO-), 146.18, 145.73 (galloyl C-3, C-5), 140.1, 140.15, 140.2,(galloyl C4), 120.5, 120, 119.2, 119.1 (galloyl, C-1), 109.19 (galloyl C-2 & C-6), 92.35 (anomeric glc. C-1), 63.24 (glc. C-6), 76.66 (glc. C-

Table 1. Tentatively assigned structures based on HPLC/ESI-MS.

Peak no.	tR (min)	Identified compound	Negative ionization MS/MS	Positive ionization MS/MS	References
1	1.92	HHDP hexoside	481.06 **301.12** 437.26 275.16	483.08 **465.16** 311.14 309.09 437.09 337.06 291.04	Mena et al., 2012
2	2.44	Galloyl quinic acid	343.07 **169.07** 299.2 191.15 173.1 125.14 328.21	345.08 **152.97** 327.17 171.09 124.99	Wyrepkowski et al., 2014
3	3.13	Ellagic acid	**301.00**, 257, 229, 185		Wyrepkowski et al., 2014
4	3.29	Digalloyl hexoside	483.08 **451**.16 313.16 331.22 301.14 271.18 169.12	485.04 **453**.17	Wyrepkowski et al., 2014
5	3.61	Digalloyl quinic acid	495.08 **343.21** 325.27 247.13 193.11 169.15		Wyrepkowski et al., 2014
6	3.88	Myricetin hexoside	479.05 **461.25** 313.19 317.17 301.14 435.18 277.1 169.09	481.10 **319.13** 463.20 421.03 309.13	Regueiro et al., 2014
7	4.37	digalloyl HHDP hexose Pedunculagin II	785.11 **633.29** 481.19 451.18 301.13 275.19		Dincheva et al., 2013; Fischer et al., 2011
8	4.66	Galloyl HHDP-hexoside	633.07 **301.13** 463.19 275.15	635.09 **617.24** 465.14 446.81 429.28 315.11 303.11 277.20	Mena et al, 2012
9	4.85	Protocatechuiic hexoside	315.07 **300.14** 153.03 270.1	317.12 **185** 155.04 203.12 299.14	Abu-Reidah et al., 2013
10	5.35	Myricetin pentoside	449.04 **317.19** 379.17 301.19 285.20 405.20 433.19 271.17 169.12		Fracassetti et al., 2013
11	10.37	Lagerstannin B derv	967.16 **483.16**	969.18 **951.23** 799.36 483.21 315.19 303.19	Fischer et al., 2011
12	10.67	Brevifolin	247.13 **203.09** 219.15 191.15 175.16	249.04 **207.05** 193.04	Wu et al., 2012
13	11.18	Galloyl HHDP hexose (Isostrictinin)	633.07 **451.12** 301.13	635.09 **617.25** 465.23 321.13 303.16 277.13	Wu et al., 2012
14	11.45	Vescalin or castalin/ tergallagic C-glucoside	631.06 **301.15** 613.17 463.21 451.15 275.17 631.06 613.17 461.13 445.22 301.15	633.07 **615.20** 471.27 427.15 309.12.	Piwowarski and Kiss, 2012
15	12.92	Valoneic acid dilactone	469 **425.15** 393.95 301.18 169.14		Wyrepkowski et al., 2014
16	13.04	Digallic acid	321.03 **169.08** 277.15 233.14 189.03 147.03 125.14		Tian et al., 2009
17	13.22	Pentagalloyl hexose	939.02 **769.23** 787.28 635.29 617.29 469.10 425.17 301.18	941.03 **453.09** 471.01 407.11 922.4	Wyrepkowski et al., 2014
18	13.27	Bis-HHDP-hexose (casuariin)	783.07 **631.22** 451.15 299.15 271.18	785.08 **449.15** 767.28 633.17 615.18 337.07 319.14 303.18 279.12 261.11	Mena et al., 2012; Fischer et al., 2011
19	14.47	Methyl gallate	183.03 **168.01**, 124.07		
20	14.67	Dimers of tergallagic-O-hexoside	631.06 **451.18** 425.17		Mena et al, 2012
21	15.05	Trigalloyl hexose	635.09 **483.23** 465.23 301.15 313.18 275.16	637.10 **466.21** 454.26 303.06	Wyrepkowski et al., 2014
22	15.18	Syringic acid hexoside	359.1 **239.14** 197.2 299.25 269.18 169.12		Abu-Reidah et al., 2013

Table 1. Contd.

23	16.21	Lagerstannin C	649.07 **435.2** 605.23 301.17 497.21	651.08 **633.21** 337.14 481.23 463.2 445.1 355.1 253.07	Fischer et al., 2011; Mena et al., 2012
24	16.53	Caffeic acid hexoside	341.09 **179.08**		Abu-Reidah et al., 2013
25	16.61	Galloyl ellagic acid	453.04 **431.31** 301.07 291.08 247.11 169.04		
26	16.93	Phyllanthusin U	924.11 **301.11** 622.25 604.22 290.21 906.25 879.27 275.16	926.12 **908.27** 606.16 588.16 571.19 774.2 454.28 436.11 303 277.12	Wu et al., 2012
27	17.50	P-coumaroyl quinic acid	337.09 **163.10** 191.15 119.21	339.11 **147.02** 320.09	Abu-Reidah et al., 2013
28	17.54	Isorh derv	445.04 **401.20** 315.25 343.2 311.14 427.22 415.34 287.26 169.12		
29	18.44	Punicalin A	781.11 **691.2** 763.31 479.19 783.34 425.26 301.25	783.07 **723.03** 765.2 553.05 277.13 303.11 463.18 445.22 613.16 631.29	Mena et al., 2012 Fischer et al., 2011
30	21.29	Galloyl shikimic acid	325.06 **173.12** 169.03 125.06		Wyrepkowski et al., 2014
31	21.46	Quinic acid	191.06 **127.07** 173.2 85.03 171.12 111.11 93.04		Simirgiotis 2013
32	21.75	Vesgalagin or castalagin	933.07 **613.21** 301.19 273.15 913.22 631.2 569.3 463.18	935.08 **783.19** 453.05 303.04 337.06	Piwowarski and Kiss, 2012
33	21.85	Gallic acid	169.01 **125.06**	171.03 **126.99** 152.99 109.03	Wyrepkowski et al., 2014
34	21.95	Phyllanthusiin B	969.09 **925.22** 949.14 881.26 633.20 589.24 419.31 301.16	971.09 **303.05** 651 335.07 951.19 479.18 315.10 277.16	Wu et al., 2012
35	23.5	Dehydrated tergallagic *C*-hexoside	613.01 **407.25** 595.18 569.26 523.22 491.32 371.16 301.2 291.22 613.01 559.14 495.24 463.24 301.21	615.06 **453.10** 291.14	Cantos et al., 2003
36	24.15	Lagerstannin B (Flavogalloyl-HHDP-gluconic acid)	949.2 **495.2** 903	951.21 **453.68** 931.45 780.23 701.51 497.13 479.28 589.29 337.15	Fisher et al, 2011
37	24.59	Phyllanthusiin C	925.10 **605.22** 301.11 623.22 551.15 453.17 881.24	927.11 **756.19** 303.10 277.13	Wu et al, 2012
38	24.67	Tellimagrandin I isomer (digalloyl-HHDP-hexose)	785.08 **301.11** 483.28 633.28 741.3 615.05	787.10 **303.06** 769.20 617.22 321.06 725.06	Wyrepkowski et al., 2014
39	24.89	Granatin A/lagerstannin A	799.16 **301.18** 479.22 781.06 635.26	801.11 **303.08** 463.2 783.23 277.11 471.07 481.22 453.21 337.16 321.16	Sentandreu et al., 2013
40	25.27	Monogalloyl hexose	331.07 **169.17** 271.12 313.14 211.23 193.06 125.18	333.08 **171.01** 315.11 153.05 127.06	Wyrepkowski et a.l, 2014
41	25.64	Ethyl gallate	197.05 **169.06** 125.1	199.06 **126.97** 170.99 137.03 152.95	Wyrepkowski et al, 2014
42	27.14	Tetragalloyl hexose	787.1 **635.22** 617..25 301.13	789.11 **771.08** 619.08 449.21 303.08	Wyrepkowski et al., 2014

Table 1. Contd.

43	28.63	Heptagalloyl hexose	1243.1 **1091.23** 939.26 917.24		Berardini et al 2004
44	30.57	Pedunculagin I isomer	783.07 **481.18** 299.18 301.1 451.15 271.2 613.15 631.23		Mena et al., 2012; Fischer et al., 2011
45	34.14	Castalgin derv	965.09 **933.18** 631.22 301.21 or 965.09 613.28 933.15 631.23 301.15	969.10 **935.2** 647.15 303.15 277.1 795.39 477.10	
46	34.73	Casuarinin/ Galloyl bis-hhdp-glucose	935.08 **633.23** 613.24 917.19 301.14	937.09 **919.17** 862.22 783.19 633.3 303.13	Liberal et al., 2014
47	34.81	Quercetin pentoside	433.04 **405.18** 291.17 303.14 389.21 269.24 301.2 275.23		Regueiro et al., 2014
48	41.16	Granatin B	951.07 **933.16** 613.22 301.22	953.08 **934.18** 783.21 633.23 615.17 465.23	Mena et al., 2012
49	42.13	Catechin or Epicatechin	289 **245.11** 291.01, 291.35		Pérez-Magariño et al.. 1999
50	43.84	Quercetin hexoside	463.05 **301.15** 343.16 373.17 275.17 169.17	465.07 **303.07** 277.09	Kajdzanoska et al., 2010
51	44.15	HHDP-trigalloyl hexose Tellimagrandin II/pterocaryanin C isomer	937.09 **633.22** 785.18 301.15	939.11 **303.07** 770.18 647.26 455.15 321.13	Regueiro et al., 2014
52	44.41	Kaempferol glucuronide hexoside	623.13 **285.17** 605.17 447.29	625.14 **287.12** 449.14	Abu-Reidah et al., 2013
53	44.61	Kaempferol	285.19 **241.16** 217.25 199.15 175.15 151.06	287.12 **269.21** 251.16 209.15 191.15	Martucci et al., 2014
54	46.70	Isorhamnetin hexoside	477.07 **315.12** 300.17	479.08 **317.10** 419.96 361.03 461.16	Hossain et al., 2010
55	46.98	Isorhamnetin	315.01 **300.15** 270.09 299.13 169.15	317.03 **285.07** 302.04 270.37	Kim and Park, 2009
56	48.55	Apigenin	269.16 **225.22** 195.12		Abu Reidah et al., 2013;
57	48.65	Apigenin 8 C-hexoside	431.10 **311.19** 341.16 269.17		Matrucci et al., 2014
58	49.0	Kaempferol 7 hexoside	447.09 **285.16** 169.17	449.11 **287.14** 429.21	Kajdzanoska et al., 2010
59	49.70	Hexagalloyl hexose	1091.12 **939.25** 940.24 787.30		Berardini et al., 2004
60	50.95	Chebulagic acid	953.08 **935.18** 907.16 787.25 739.31 617.35 613.25 301.16	955.10	Huang et al., 2011; Wu et al., 2012
61	51.01	Dehydrogalloyl-HHDP-hexoside	615.06 **463.22** 301.18 257 229	617.08 **303.08** 277.07 455.13 429.01	Mena et al., 2012
62	51.21	Myricetin	317.20 **289.19** 300.12 302.20 243.18 245.18 209.14	319.04 **301.1** 291.09 273.11 245.06	Sójka et al., 2009
63	52.51	Pentagalloyl HHDP hexose	1241.12 **1087.34** 937.19 769.12 787 633.31 469.18		
64	54.03	Apigenin 7 hexoside	431.10 **269.21** 413.13 311.20 275.12		Abu-Reidah et al., 2013

Ions in bold indicate the most intense product ion (100% relative intensity). Ions are arranged according to their relative abundance.

5), 76.65 (glc. C-3), 72.1 (glc. C-2), 67 (glc. C-4), 63.24 (glc.C-6). Methyl gallate (2), cream colored needles, Rf values 0.72 (S1), 0.58(S2) on PC. It

Table 2. *N. alba* rhizome AEE against different standard microorganisms.

Organism tested	Zone of inhibition (mm)			
	***N. alba* AEE**	**Ofloxaciline**	**AMP B***	**AMP B***
Staphylococcus aureus (ATCC 6538)	21±00	32±00	-	-
Bacillus subtilis (ATCC 6633)	10±01	36±00	-	-
Sarcina lutea (*ATCC* 9341)	18±05	30±03	-	-
Escherichia coli (ATCC 8739)	12±00	29±00	-	-
Proteus vulgaris (ATCC 6899)	10±00	38±02	-	-
Salmonella typhimurium (ATCC 13311)	15±00	27±00	-	-
Shigella sonni (*ATCC* 9290)	12±05	31±00	-	-
Pseudomonas aeruginosa (ATCC 27853)	12±02	29±05	-	-
Candida albicans (ATCC 10231)	12±01	-	25±05	25±05

*AMP B: Amphotericin B; No results means test not done.

Table 3. Minimum inhibitory concentrations (MIC) of *N. alba* rhizome AEE against standard microbial strains.

Standard strain	MIC (mg/mL)
S. aureus (ATCC 6538)	0.25
B. subtilis (ATCC 6633)	>2
E. coli (ATCC 8739)	>2
P. aeruginosa (ATCC 27853)	>2
C. albicans (ATCC 10231)	>2

gave violet blue color using short UV light and intense blue color with $FeCl_3$. UV λ_{max} (nm): (MeOH) 218, 272.^{1}H-NMR (300 MHz, DMSO-d_6): δ 6.96 (2H, *s*, H-2 & H-6), δ 3.39 (3H, s, OOCH3).

Ethyl gallate (3), white amorphous powder, Rf values 0.9 (S1), 0.72 (S2) on PC. It gave violet blue color using short UV light and intense blue color with $FeCl_3$. UV λ_{max} (nm): (MeOH) 225, 274. ^{1}H-NMR (300 MHz, DMSO-d_6): δ ppm 6.93 (2H, *s*, H-2 & H-6), 4.20 (2H, *q*, J=7 Hz, CH_2), 1.26 (3H, *t*, J=7 Hz, CH_3). Gallic and ellagic acid have been tentatively identified by Co-chromatography.

Antimicrobial activity by disc diffusion test

The sensitivity of nine standard strains to extracts from *N. alba* rhizomes was tested using disc diffusion method. All standard bacterial strains used were sensitive to ofloxacin while *C. albicans* was sensitive to amphotericin B. Both *S. aureus* and *Sarcina lutea* showed the highest sensitivity to *N. aba* rhizome extract as shown in Table 2.

Minimum inhibitory concentrations of *N. alba* rhizome extract and isolated compounds

The MIC of rhizome extract was equivalent to 0.25 mg/mL for standard *S. aureus* and above 2 mg/mL with standard strains of *B. subtilis, E. coli, P. aeruginosa and C. albicans* (Table 3 to 5).

Standard *S. aureus* was chosen for next studies in addition to the four clinical strains. *N. alba* extract showed high activity against Standard *S. aureus* and clinical isolates except Staph (3) isolate. Methyl gallate showed the highest activity against all tested microorganisms compared to ethyl gallate and pentagalloyl glucose.

The effect of *N. alba* extract and pure compounds on biofilm formations was studied. The minimum concentration that causes inhibition of growth was used. Methyl gallate caused a significant reduction in biofilm formation (84.9%) followed by the rhizome extract (78.8%) ($P<0.01$). Both standard strain and the clinical isolate Staph (2) were the most affected by the extract and methyl gallate followed by isolate Staph (3). The degree of inhibition was not correlated with the MIC of extract or the pure component on different tested microorganisms. Pentagalloyl glucose showed the least effect on biofilm formation. Methyl gallate showed the best antimicrobial and anti-biofilm activity in agreement with previous reports (Kang et al., 2008). This activity was attributed to its structure; a lipophilic alkyl chain at one end is connected via an ester linkage to the galloyl group bearing the polar hydroxyl groups at the other end. This amphiphilic property makes the cell membrane of *S. aureus* one of the most likely target sites of the action of alkyl gallate (Shibata et al., 2005). The antibacterial effect of alkyl gallate is due to, both, membrane disruption and affecting cell division by anti-FtsZ activity (Król et al.,

Table 4. Minimum Inhibitory Concentrations (MIC) of *N. alba* rhizome AEE and its main constituents against *S. aureus* standard strain and clinical isolates.

Microorganism	MIC (mg/mL)			
	***N. alba* AEE**	**Methyl gallate**	**Ethyl gallate**	**Pentagalloyl glucose**
Staph. aureus (ATCC 6538)	0.25	0.1	>0.1	>0.1
Staph 1	0.5	0.1	>0. 1	>0. 1
Staph 2	0.25	0.1	>0.1	>0. 1
Staph 3	2	0.1	>0.1	>0. 1
Staph 4	0.5	0.1	>0. 1	>0. 1

Table 5. Percentage reduction in biofilm formation of *Staphylococcus aureus* by *N. alba* rhizome AEE and its main constituents at MIC.

Microorganism	Percentage reduction in biofilm formation (%)			
	***N. alba* AEE**	**Methyl gallate**	**Ethyl gallate**	**Pentagalloyl glucose**
S. aureus (ATCC 6538)	78.84	84.9	62.8	19.28
Staph 1	24.40	51.67	44.49	48.32
Staph 2	77.41	85.6	73.49	10
Staph 3	70.00	80	9.3	43.35
Staph 4	4.80	66	12.72	8.78

2015). Their antibacterial mode of action was also suggested to be as surface-active agents affecting membrane integrity and hence affect biofilm formation (Takai et al., 2011).

1, 2, 3, 4, 6-penta-*O*-galloyl-β-D-glucose (β-PGG) is a prototypical gallotannin and the central compound in the biosynthetic pathway of hydrolysable tannin. β-PGG has five ester bonds formed between carboxylic groups of gallic acids and aliphatic hydroxyl groups of the glucose core. It is present in a number of medicinal herbals such as *Rhus chinensis* Mill and *Paeonia suffruticosa* and showing several biological activities (Zhang et al., 2009). In our study, PGG showed lower activity compared with methyl and ethyl gallate.

Radical scavenging activity

Methyl gallate showed the best radical scavenging activity with IC_{50} 3±0.36 µg/mL followed by ethyl gallate 4.7±0.23 µg/mL while IC_{50} of pentagalloyl glucose was 12±0.54 µg/mL compared with vitamin C 12±3.5 µg/mL. Antioxidant activity of methyl and ethyl gallate was proved by Wang et al. (2014) and Kalaivani et al. (2011), respectively. While moderate activity of ethyl gallate was previously reported by Kalaivani et al. (2011)

Other report showed that PGG showed an EC_{50} of scavenging 1, 1-diphenyl-2-picrylhydrazil (DPPH) free radical at about 1 µg/mL (1.1 µM) in test tubes, which was more potent than vitamin E (Abdelwahed et al., 2007).

Cytotoxic activity

In term of antiproliferative/cytotoxic IC_{50} values, Methyl gallate showed the highest activity against HepG2- cell line with IC_{50}= 9.61±0.3 µg/ml, while ethyl gallate and pentagalloyl glucose values were 41.9±0.23 and 41.2±0.41 µg/ml, respectively compared with Doxorubicin 0.56 µg/ml, standard cytotoxic.

PGG cytotoxic activity against hepatocellular carcinoma was comparable to ethyl gallate with IC_{50} 41.2 and 41.9 µg/ml, respectively. This was in agreement with Oh et al. (2001) who isolated PGG from the root of *Paeonia suffruticosa* and tested its *in vitro* effect on human hepatocellular carcinoma SK-HEP-1 cells. Up to 50 µM PGG inhibited the growth of SK-HEP-1 cells in a dose-dependent fashion and 30 µM PGG significantly induced G1 arrest.

Conclusion

This study is the first report for the identification and characterization of phenolic constituents in *N. alba* rhizomes and evaluation of its anti-biofilm and cytotoxic activities. *N. alba* rhizomes revealed a promising anti-biofilm activity with suggested contribution in antibacterial therapy.

Conflict of Interest

The authors declare that there are no conflicts of interest.

ACKNOWLEDGEMENT

The authors are thankful to L.A. Mahmoud Omar for providing the plant material.

REFERENCES

Abdelwahed A, Bouhlel I, Skandrani I, Valenti K, Kadri M, Guiraud P, Steiman R, Mariotte AM, Ghedira K, Laporte F, Dijoux-Franca MG, Chekir-Ghedira L (2007). Study of antimutagenic and antioxidant activities of gallic acid and 1,2,3,4,6-pentagalloylglucose from *Pistacia lentiscus*. Confirmation by microarray expression profiling. Chem. Biol. Interact. 165:1-13.

Abu-Reidah IM, Arráez-Román D, Segura-Carretero A, Fernández-Gutiérrez A (2013). Extensive characterisation of bioactive phenolic constituents from globe artichoke (*Cynara scolymus L.*) by HPLC–DAD-ESI-QTOF-MS. Food chem. 141(3):2269-2277.

Archer NK, Mazaitis MJ, Costerton JW, Leid JG, Powers ME, Shirtliff ME (2011). *Staphylococcus aureus* biofilms: Properties, regulation and roles in human disease. Virulence 2:445-459.

Barry KM, Davies NW, Mohammed CL (2001). Identification of hydrolysable tannins in the reaction zone of Eucalyptus nitens wood by high performance liquid chromatography--electrospray ionisation mass spectrometry. Phytochem. Anal. 12(2):120-127.

Berardini N, Carle R, Schieber A (2004). Characterization of gallotannins and benzophenone derivatives from mango (*Mangifera indica L.* cv. 'Tommy Atkins') peels, pulp and kernels by high-performance liquid chromatography/electrospray ionization mass spectrometry. Rapid Commun. Mass Spectrum 18:2208-2216.

Bose A, Ray S, Sahoo M (2013). Central depressant activity of ethanol extract of *Nymphaea alba* rhizome in mice. Orient. Pharm. Exp. Med. 13:159-64.

Bose AS, Moumita SR, Sudhanshu SC (2014). Uterotonic properties of *Nymphaea alba* on isolated myometrium model. Int. J. Pharm.Pharm. Sci. 6:490-493.

Bose AS, Ray S (2012a). *In vivo* evaluation of anti-diarrheal activity of the rhizome of *Nymphaea alba* (Nymphaeaceae). Orient. Pharm. Exp. Med. 12:129-134.

Bose AS, Sahoo M (2012b). Evaluation of analgesic and antioxidant potential of ethanolic extract of *Nymphaea alba* rhizome. Oxid. Antioxid. Med. Sci. 1:217-223.

Cantos E, Espín JC, López-Bote C, Ordóñez JA, Tomás-Barberán FA (2003). Phenolic Compounds and Fatty Acids from Acorns (Quercus spp.), the Main Dietary Constituent of Free-Ranged Iberian Pigs. J. Agric. Food Chem. 51:6248-6255.

Cheesbrough M (2005). *District Laboratory Practice in Tropical Countries,* 2nd edition, New York, Cambridge University Press.

Dincheva I, Badjakov I, Kondakova V, Dobson P, Mcdougall G, Stewart D (2013). Identification of the phenolic components in Bulgarian raspberry Cultivars by LC-ESI-MS. IJASR 3:127-138.

Elegami AA, Bates C, GraY AI, Mackay SP, Skellern GG, Waigh RD (2003). Two very unusual macrocyclic flavonoids from the water lily *Nymphaea lotus*. Phytochemistry 63:727-731..

Fischer UA, Carle R, Kammerer DR (2011). Identification and quantification of phenolic compounds from pomegranate (*Punica granatum* L.) peel, mesocarp, aril and differently produced juices by HPLC-DAD–ESI/MSn. Food Chem, 127:807-821.

Fotakis G, Timbrell JA (2006). *In vitro* cytotoxicity assays: comparison of LDH, neutral red, MTT and protein assay in hepatoma cell lines following exposure to cadmium chloride. Toxicol. Lett. 160(2):171-177.

Fracassetti D, Costa C, Moulay L, Tomás-Barberán FA (2013). Ellagic acid derivatives, ellagitannins, proanthocyanidins and other phenolics, vitamin C and antioxidant capacity of two powder products from camu-camu fruit (*Myrciaria dubia*). Food Chem. 139:578-588.

Gilani AH, Rahman AU (2005). Trends in ethnopharmacology. J. Ethnopharmacol. 100:43-49.

Hassaan Y, Handoussa H, El-Khatib AH, Linscheid MW, El Sayed N, Ayoub N (2014). Evaluation of Plant Phenolic Metabolites as a Source of Alzheimer's Drug Leads, BioMed Research International, 2014. Article ID 843263. 10 p.

Hossain MB, Rai DK, Brunton NP, Martin-Diana AB, Barry-Ryan C (2010). Characterization of Phenolic Composition in Lamiaceae Spices by LC-ESI-MS/MS. J. Agric. Food Chem. 58:10576-10581.

Huang ST, Wang CY, Yang RC, Wu HT, Yang SH. (2011). Ellagic Acid, the Active Compound of *Phyllanthus urinaria*, Exerts In Vivo Anti-Angiogenic Effect and Inhibits MMP-2 Activity. Evid. Based. Complement. Alternat. Med. 2011:215035.

Jambor J, Skrzypczak LA (1991). Phenolic acids from the flowers of *Nymphaea alba* L. Acta Soc. Bot. Pol. 60:127-132.

Jones SM, Morgan M, Humphrey TJ, Lappin-Scott H (2001). Effect of vancomycin and rifampicin on meticillin-resistant *Staphylococcus aureus* biofilms. Lancet 357:40-41.

Kajdzanoska M, Gjamovski V, Stefova M (2010). HPLC-DAD-ESI-MS Identification of phenolic compounds in cultivated strawberries from Macedonia. Maced. J. Chem. Chem. Eng. 29:181-94.

Kalaivani T, Rajasekaran C, Mathew L (2011). Free radical scavenging, cytotoxic, and hemolytic activities of an active antioxidant compound ethyl gallate from leaves of *Acacia nilotica* (L.) Wild. Ex. Delile subsp. indica (Benth.) Brenan. J Food Sci. 76:144-149.

Kang MS, Oh JS, Kang IC, Hong SJ, Choi CH. (2008). Inhibitory effect of methyl gallate and gallic acid on oral bacteria. J. Microbiol. 46:744-750.

Khan N, Sultana S (2005). Inhibition of potassium bromate-induced renal oxidative stress and hyperproliferative response by *Nymphaea alba* in Wistar rats. J. Enzyme Inhib. Med. Chem. 20:275-283.

Khanbabaee K, Vanree T (2001). Tannins: classification and definition. Nat. Prod. Rep. 18:641-649.

Kim H, Park SH (2009). Metabolic profiling and discrimination of two Cacti cultivated in Korea using HPLC-ESI-MS and multivariate statistical analysis. J. Korean Soc. Appl. Biol. Chem. 52:346-352.

Klancnik A, Piskernik S, Jersek B, Mozina SS. (2010). Evaluation of diffusion and dilution methods to determine the antibacterial activity of plant extracts. J. Microbiol. Methods 81:121-126.

Kosalec I, Bakmaz M, Pepeljnjak S, Vladimir-Knezevic S (2004). Quantitative analysis of the flavonoids in raw propolis from northern Croatia. Acta Pharm. 54:65-72.

Król E, Desousa A, Dasilva I, Polaquini CR, Regasini LO, Ferreira H, Scheffers D (2015). Antibacterial activity of alkyl gallates is a combination of direct targeting of FtsZ and permeabilization of bacterial membranes. Front. Microbiol. 6:390.

Lee TH, Chiou JL, Lee CK, Kuo YH (2005). Separation and Determination of Chemical Constituents in the Roots of *Rhus Javanica* L. Var. Roxburghiana. J. Chin. Chem. Soc. 52:833-841.

Li XC, Elsohly HN, Hufford CD, Clark AM (1999). NMR assignments of ellagic acid derivatives. Magn. Reson. Chem. 37:856-859.

Liberal J, Francisco V, Costa G, Figueirinha A, Amaral MT, Marques C, Girão H, Lopes MC, Cruz MT, Batista MT (2014). Bioactivity of *Fragaria vesca* leaves through inflammation, proteasome and autophagy modulation. J. Ethnopharmacol. 158:113-122.

Martucci MEP, De Vos RCH, Carollo CA, Gobbo-Neto L. (2014). Metabolomics as a Potential Chemotaxonomical Tool: Application in the Genus Vernonia Schreb. PLoS One. 9(4): e93149.

Mena P, Calani L, Asta CD, Galaverna G, García-Viguera C, Bruni R, Crozier A, Del Rio D (2012). Rapid and Comprehensive Evaluation of (Poly)phenolic Compounds in Pomegranate (*Punica granatum* L.) Juice by UHPLC-MSn. Molecules 17:14821-14840.

Nawwar MAM, Hussein SAM, Merfort I (1994). NMR spectral analysis of polyphenols from *Punica granatum*. Phytochemistry, 36:793-798.

Nonaka GI, Ishimatsu M, Tanaka T, Nishioka I, Nishizawa M (1987). Tannins and Related Compounds. LVIII.: Novel Gallotannins Possessing an α-Glucose Core from *Nuphar japonicum* DC.(Organic,Chemical). Chem. Pharm. Bull. 35:3127-3131.

Oh GS, Pae HO, Oh H, Hong SG, Kim IK, Chai KY, Yun YG, Kwon TO, Chung HT (2001). In vitro anti-proliferative effect of 1,2,3,4,6-penta-O-galloyl-beta-D-glucose on human hepatocellular carcinoma cell line, SK-HEP-1 cells. Cancer Lett. 174:17-24.

Oktay M, Gülçin İ, Küfrevioğlu Öİ (2003). Determination of in vitro antioxidant activity of fennel (*Foeniculum vulgare*) seed extracts. LWT-Food Sci. Technol. 36:263-271.

Otto M (2009). *Staphylococcus epidermidis* – the “accidental” pathogen. Nat. Rev. Microbiol. 7:555-567.

Peeters E, Nelis HJ, Coenye T (2008). Resistance of planktonic and biofilm-grown *Burkholderia cepacia* complex isolates to the transition metal gallium. J. Antimicrob. Chemother. 61:1062-1065.

Pérez-Magariño S, Revilla I, González-SanJosé ML, Beltrán S (1999). Various applications of liquid chromatography–mass spectrometry to the analysis of phenolic compounds. J. Chromatogr. A. 847:75-81.

Piwowarski JP, Kiss AK (2013). C-glucosidic ellagitannins from *Lythri herba* (European Pharmacopoeia): Chromatographic profile and structure determination. Phytochem. Anal. 24(4):336-348.

Regueiro J, Sánchez-González C, Vallverdú-Queralt A, Simal-Gándara J, Lamuela-Raventós R, Izquierdo-Pulido M (2014). Comprehensive identification of walnut polyphenols by liquid chromatography coupled to linear ion trap–Orbitrap mass spectrometry. Food Chem. 152:340-348.

Rios JL, Recio MC (2005). Medicinal plants and antimicrobial activity. J. Ethnopharmacol. 100:80-84.

Sauer K, Camper AK (2001). Characterization of phenotypic changes in *Pseudomonas putida* in response to surface-associated growth. J. Bacteriol. 183:6579-6589.

Saura-Calixto F, Pérez-jiménez J (2009). Tannins: Bioavailability and Mechanisms of Action. *Chemoprevention of Cancer and DNA Damage by Dietary Factors.* Wiley-VCH Verlag GmbH & Co. KGaA.

Seeram NP, Lee R, Scheuller HS, Heber D (2006). Identification of phenolic compounds in strawberries by liquid chromatography electrospray ionization mass spectroscopy. Food Chem. 97:1-11.

Sellappan S, Akoh CC (2002). Flavonoids and antioxidant capacity of Georgia-Grown Vidalia onions. J. Agric. Food Chem*,* 50:5338-42.

Sentandreu E, Cerdán-Calero M, Sendra JM (2013). Phenolic profile characterization of pomegranate (*Punica granatum*) juice by high-performance liquid chromatography with diode array detection coupled to an electrospray ion trap mass analyzer. J. Food Compos. Anal. 30:32-40.

Shibata H, Kondo K, Katsuyama R, Kawazoe K, Sato Y, Murakami K, Takaishi Y, Arakaki N, Higuti T (2005). Alkyl gallates, intensifiers of beta-lactam susceptibility in methicillin-resistant *Staphylococcus aureus*. Antimicrob. Agents Chemother. 49:549-555.

Shimada K, Fujikawa K, Yahara K, Nakamura T (1992). Antioxidative properties of xanthan on the autooxidation of soybean in cyclodextrin emulsion. J. Agric. Food Chem. 40:945-948.

Simirgiotis MJ (2013). Antioxidant Capacity and HPLC-DAD-MS Profiling of Chilean Peumo (*Cryptocarya alba*) Fruits and Comparison with German Peumo (*Crataegus monogyna*) from Southern Chile. Molecules 18:2061-2080.

Sójka M, Guyot S, Kołodziejczyk K, Król B, Baron A (2009). Composition and properties of purified phenolics preparations obtained from an extract of industrial blackcurrant (*Ribes nigrum L*.) pomace ISAFRUIT Special Issue. J. Hortic. Sci. Biotechnol. pp. 100-106.

Takai E, Hirano A, Shiraki K (2011). Effects of alkyl chain length of gallate on self-association and membrane binding. J Biochem. 150:165-171.

Tian F, Li B, Ji B, Zhang G, Luo Y (2009). Identification and structure–activity relationship of gallotannins separated from Galla chinensis. LWT - Food Sci. Technol. 42:1289-1295.

Upadhyay A, Upadhyaya I, Kollanoor-Johny A, Venkitanarayana K (2014). Combating pathogenic microorganisms using plant-derived antimicrobials: a minireview of the mechanistic basis. BioMed Res. Int. 2014:761741.

Valentino MD, Foulston L, Sadaka A, Kos VN, Villet RA, Santamaria JJR., Lazinski DW, Camilli A, Walker S, Hooper DC, Gilmore MS (2014). Genes contributing to *Staphylococcus aureus* fitness in abscess- and infection-related ecologies. MBio. 5(5):e01729-14.

Valgas C, Souza SMD, Smânia EFA, Smânia JRA (2007). Screening methods to determine antibacterial activity of natural products. Braz.. J. Microbiol. 38:369-380.

Wang CR, Zhou R, Ng TB, Wong JH, Qiao WT, Liu F (2014). First report on isolation of methyl gallate with antioxidant, anti-HIV-1 and HIV-1 enzyme inhibitory activities from a mushroom (*Pholiota adiposa*). Environ. Toxicol. Pharmacol. 37:626-637.

Wiersema JH (1987). A monograph of *Nymphaea* subgenus Hydrocallis (Nymphaeaceae). Syst. Bot. Monogr. 16:1-112.

Wilson A (2000). *Cytotoxicity and viability assays in animal cell culture: A Practical Approach,* 3rd ed*.*, Oxford University Press.

Wu HY, Lin TK, Kuo HM, Huang YL, Liou CW, Wang PW, Chuang JH (2012). *Phyllanthus urinaria* Induces Apoptosis in Human Osteosarcoma 143B Cells via Activation of Fas/FasL- and Mitochondria-Mediated Pathways 2012: Article ID 925824. J. Evidence-Based Complementary Altern. Med. 13 p.

Wyrepkowski CC, Costa DL, Sinhorin AP, Vilegas W, DeGrandis RA, Resende FA, Varanda EA, DosSantos LC (2014). Characterization and quantification of the compounds of the ethanolic extract from *Caesalpinia ferrea* stem bark and evaluation of their mutagenic activity. Molecules 19:16039-16057.

Yassien M, Khardori N. (2004). Biofilms formation by *Staphylococcus epidermidis* modulation by fluoroquinolones. Egy. J. Biomed. Sci. 16:1-20.

Zhang J, Li L, Kim S, Hagerman A, Lu J (2009). Anti-cancer, anti-diabetic and other pharmacologic and biological activities of penta-galloyl-glucose. Pharm. Res. 26:2066-2080.

Journal of
Medicinal Plant Research

Related Journals Published by Academic Journals

- *African Journal of Pharmacy and Pharmacology*
- *Journal of Dentistry and Oral Hygiene*
- *International Journal of Nursing and Midwifery*
- *Journal of Parasitology and Vector Biology*
- *Journal of Pharmacognosy and Phytotherapy*
- *Journal of Toxicology and Environmental Health Sciences*

academicJournals